+Supplementary information for

Nickel(II) Complexes of Halogen-Containing NNO Donor Aroylhydrazones as Potential Putative Binders against SARS Cov-2 M^{pro}

Pramod Kumar Maniyampara,[a] M. Bhagiyalakshmi,[*a] M.R. Prathapachandra Kurup,[*a] E. Manoj,[b] Krishna K. Damodaran[c], M. Sithambaresan[d] and Firasat Hussain[e]

[a.] *Department of Chemistry, School of Physical Science, Central University of Kerala, Tejaswini Hills, Periye, Kasaragod 671 320, Kerala, India*

[b.] *Department of Applied Chemistry, Cochin University of Science and Technology, Kochi 682022, Kerala, India*

[c.] *Department of Chemistry, Science Institute, University of Iceland, Dunhagi 3, 107 Reykjavik, Iceland*

[d.] *Department of Chemistry, Faculty of Science, Eastern University, Chenkalady, Sri Lanka*

[e.] *Department of Chemistry, University of Delhi, Faculty of Science, North Campus, Delhi 110007, India*

Analytical data of the complexes

$[Ni(BpB)_2]$ (**1**). Yield: 62% (0.40 g); Anal. Calc. for $C_{38}H_{28}Br_2N_6O_2Ni$: C 55.72; H 3.44; N 10.26%; found: C 54.84; H 3.22; N 9.95%; Selected IR bands (KBr, ν/cm^{-1}): ν(C–O) 1353; ν(C=N) 1590, 1577; ν(N–N) 1136; Molar conductivity (Λ_m) ≈ 0 $\Omega^{-1}cm^2mol^{-1}$ in 10^{-3} M DMF at 298 K. $[Ni(BpB)(HBpB)]NO_3$ (**2**). Yield: 74% (0.50 g); Anal. Calc. for $C_{38}H_{27}Br_2N_7O_5Ni$: C 51.86; H 3.09; N 11.14%; found: C 51.52; H 2.94; N 11.36%; Selected IR bands (KBr, ν/cm^{-1}): ν(N–H) 3375; ν(C–O) 1361; ν(C=N) 1589, 1575; ν(C=O) 1614; Molar conductivity (Λ_m) ≈ 66 $\Omega^{-1}cm^2mol^{-1}$ in 10^{-3} M DMF at 298 K. $[Ni(BpB)(HBpB)]Cl$ (**3**). Yield: 72% (0.39 g), Anal. Calc. for $C_{38}H_{27}Br_2ClN_6O_2Ni$: C 53.47; H 3.19; N 9.84%; found: C 54.07; H 3.31; N 9.80%. Selected IR bands (KBr, ν/cm^{-1}): ν(N–H) 3337; ν(C–O) 1354; ν(C=N) 1588, 1574; ν(C=O) 1612; Molar conductivity (Λ_m) ≈ 75 $\Omega^{-1}cm^2mol^{-1}$ in 10^{-3} M DMF at 298 K. $[Ni(BpB)(HBpB)]Br$ (**4**). Yield:

76% (0.47 g); Anal. Calc. for $C_{38}H_{27}Br_3N_6O_2Ni$: C 50.88; H 2.92; N 8.11%; found: C 51.15; H 2.97; N 8.23%; Selected IR bands (KBr, ν/cm^{-1}): ν(N–H) 3360; ν(C–O) 1354; ν(C=O) 1613; ν(C=N) 1588, 1574; Molar conductivity (Λ_m) ≈ 77 $\Omega^{-1}cm^2mol^{-1}$ in 10^{-3} M DMF at 298 K. [Ni(DpB)$_2$] (**5**). Yield: 71% (0.47 g); Anal. Calc. for $C_{36}H_{24}Br_2N_8O_2Ni$: C 52.79; H 2.95; N 13.68%; found: C 53.15; H 2.97; N 13.55%; Selected IR bands (KBr, ν/cm^{-1}): ν(C–O) 1360; ν(C=N) 1580, 1574; Molar conductivity (Λ_m) ≈ 6 $\Omega^{-1}cm^2mol^{-1}$ in 10^{-3} M DMF at 298 K. [Ni(DpB)(HDpB)]NO_3 (**6**). Yield: 68% (0.43 g); Anal. Calc. for $C_{36}H_{25}Br_2N_9O_5Ni$: C 49.02; H 2.86; N 14.29%; found: C 49.15; H 2.97; N 14.23%; Selected IR bands (KBr, ν/cm^{-1}): ν(N–H) 3259; ν(C–O) 1358; ν(C=O) 1627; ν(C=N) 1590, 1575; Molar conductivity (Λ_m) ≈ 71 $\Omega^{-1}cm^2mol^{-1}$ in 10^{-3} M DMF at 298 K.

Table S1. Hydrogen bonding interactions in complexes **1**-**6**

Hydrogen bonding interactions

D–H···A	d(D–H) (Å)	d(H···A) (Å)	d(D···A) (Å)	<(DHA) (°)
		1		
C(2)–H(2)···N(6)#1	0.95	2.60	3.468(3)	151.6
#1 -x+1,-y+1,-z+1				
		2		
C(19)–H(19)···O(5)#1	0.93	2.54	3.2733	136
C(18)–H(18)···O(3)#1	0.93	2.47	3.353(5)	158.4
C(27)–H(27)···O(3)	0.93	2.49	3.2523	139
N(6)–H(6)···O(4)#2	0.88(4)	2.55(4)	3.065(5)	118(3)
N(6)–H(6)···O(5)#2	0.88(4)	1.82(4)	2.690(4)	171(4)
#1 -x+1,-y+1,-z+1, #2=1-x,-y,-z				
		3		
N(6)–H(6)···Cl(1)	0.877(10)	2.21(3)	3.041(5)	157(7)
C(38)–H(38)···O(2)#1	0.93	2.59	3.3158(2)	135
#1=1-x,1-y,1-z				
		4a		
O(1S)–H(1A)···Br(5)$^{\#1}$	0.82(4)	2.64(5)	3.407(5)	157(4)
N(6)–H(6)···Br(5)$^{\#2}$	0.80(5)	2.44(5)	3.167(6)	152(4)
C(34)–H(34)···O(3)$^{\#1}$	0.95	2.52	3.253(8)	134
C(72)–H(72)···O(1)$^{\#3}$	0.95	2.60	3.325(8)	134
#1=1-x,-1/2+y,1-z, #2= 2-x,-1/2+y,1-z, #3= 1-x,1/2+y,1-z				
		5a		
O(3C)–H(3A^C)···O(2)	0.84(6)	2.21(7)	3.035(6)	170(7)
C(11B^B)–	0.95	2.18	3.068(6)	155

H(11B^B)···O(3C)[#1]				
C(3)–H(3)···O(2)[#2]	0.95	2.58	3.425(3)	148
C(14)–H(14)···N(4)	0.95	2.40	2.728(4)	100
C(22)–H(22)···N(6)	0.95	2.62	3.070(4)	109
C(29)–H(29)···N(8)	0.95	2.62	2.942(4)	100
C(32)–H(32)···N(8)	0.95	2.42	2.747(3)	100
#1 1-x,1-y,1-z, #2=-x,1-y,1-z				
		6		
N(8)–H(8')···O(5) #1	0.88	1.90	2.7534(3)	164
C(14)–H(14)···O(5) #2	0.93	2.54	3.3277(3)	143
C(15)–H(15)···O(4) #2	0.93	2.48	3.3239(3)	151
C(26)–H(26)···O(4) #3	0.93	2.49	3.2658(3)	141
C(32)–H(32)···O(1) #4	0.93	2.58	3.2541(3)	129
#1= 1/2-x,1/2+y,3/2-z #2=1/2+x,1/2-y,-1/2+z #3=-1/2+x,1/2-y,-1/2+z #4=1-x,1-y,1-z				
D = donor, A = acceptor.				

Table S2. π···π interactions in complex **1, 5a** and **6**

π···π interactions					
Cg(I)···Cg(J)	**Cg···Cg (Å)**	**α (°)**	**β (°)**	**γ (°)**	**Slippage**
		1			
Cg(7)···Cg(10)[#1]	3.8909(3)	8	32.7	27.1	2.100
Cg(10)···Cg(7)[#1]	3.8909(3)	8	27.1	32.7	1.772
#1=1-x,-y,-z					
Cg(7)=C(7)–C(8)–C(9)–C(10)–C(11)–C(12), Cg(10)=C33–C34–C35–C36–C37–C38					
		5a			
Cg5···Cg5[#1]	3.6600(14)	0.00(12)	22.7	22.7	1.415
Cg5···Cg10[#2]	3.6856(16)	3.98(12)	21.2	18.4	1.332
Cg8···Cg8[#3]	3.9238(16)	0.02(13)	25.8	25.8	1.711
Cg10···Cg5[#4]	3.6855(16)	3.98(12)	18.4	21.2	1.162
#1= -x,1-y,1-z, #2= -1+x,y,z, #3= -x,-y,1-z, #4= 1+x,y,z.					
Cg(5)= N(1)–C(1)–C(2)–C(3)–C(4)–C(5), Cg(8)= N(6)–C(25)–C(26)–C(27)–C(28)–C(29), Cg(10)= C(13)–C(14)–C(15)–C(16)–C(17)–C(18).					
		6			
Cg(1)–Cg(7)	3.9677(4)	83	29.4	72.3	
Cg(5)= N(1)–C(1)–C(2)–C(3)–C(4)–C(5), Cg(7)= N(5)–C(19)–C(20)–C(21)–C(22)–C(23)					
Cg = centroid; α = dihedral angles between planes I and J; β = angle between Cg–Cg and Cg(J)_perp; γ = angle between Cg–Cg and Cg(I)_perp.					

Table S3. C–H···π and Y–X···π interactions and interactions in complexes **1**-**6**

C–H···Cg/C–Br···Cg	H···Cg/X···Cg (Å)	C···Cg/Y···Cg (Å)	C–H···Cg/Y–X···Cg (°)
	1		
C(3)–H(3)···Cg(9)	2.63	3.4999(3)	55
C(27)–H(27)···Cg(7)$^{\#1}$	2.88	3.7835(3)	51
C(28)–H(28)···Cg(1) $^{\#1}$	2.83	3.5310(3)	39
C(36)–Br(2)···Cg(6) $^{\#2}$	3.5512(3)	5.4095(4)	165.11(1)
C(36)–Br(2)···Cg(10)$^{\#3}$	3.6953(3)	4.2180(3)	92.14(1)
#1=-1+x,y,z, #2=1/2-x,-1/2+y,1/2-z, #3=1-x,-y,1-z.			
	2		
N(7)–O(3)···Cg(4)	3.8834	4.9827	149
N(7)–O(5)···Cg(9)$^{\#1}$	3.3379	4.4678	149
C(17)–Br(1)···Cg(3)$^{\#2}$	3.8098	4.5647	101
#1=1-x,-y,-z ,#2=-1/2+x,1/2-y,1/2+z.			
	3		
C(1)–H(1)···Cg(2)	2.91	3.265(6)	104
C(20)–H(20)···Cg(1)	2.85	3.167(6)	101
C(17)–Br(1)···Cg(3)$^{\#1}$	3.8302(18)	4.475(4)	97.03(13)
#1=-1/2+x,1/2-y,1/2+z			
	4a		
C(17)–Br(1)···Cg(5)$^{\#1}$	3.975(3)	4.059(7)	79.0(2)
C(17)–Br(1)···Cg(13)	3.806(2)	4.417(7)	96.1(2)
C(55)–Br(3)···Cg(3)$^{\#2}$	3.760(2)	4.463(6)	99.21(17)
#1= -1+x,y,z, #2= -1+x,y,1+z			
Cg(1)=Ni(1)–O(1)–C(13)–N(3)–N(2), Cg(2)=Ni(1)–O(2)–C(32)–N(6)–N(5), Cg(3)=Ni(1)–N(1)–C(5)–C(6)–N(2), Cg(4)=Ni(1)–N(4)–C(24)–C(25)–N(5), Cg(5)= N(1)–C(1)–C(2)–C(3)–C(4)–C(5), Cg(6)=N(4)–C(20)–C(21)–C(22)–C(23)–C(24), Cg(7)=C(7)–C(8)–C(9)–C(10)–C(11)–C(12), Cg(9)=C(26)–C(27)–C(28)–C(29)–C(30)–C(31), Cg(10)=C(33)–C(34)–C(35)–C(36)–C(37)–C(38), Cg(13)= Ni(2)–N(7)–C(43)–C(44)–N(8).			
	5a		
C(1)–H(1)···Cg(2)	2.85	3.136(3)	24
C(19)–H(19)···Cg(1)	2.72	3.135(2)	18
C(21)–H(21)···Cg(10)$^{\#1}$	2.66	3.514(3)	64
C(29)–H(29)···Cg(2)$^{\#2}$	2.94	3.832(3)	52
C(16)–Br(1)···Cg(3)$^{\#3}$	3.8582(9)	4.274(3)	10.93
C(16)–Br(1)···Cg(7)$^{\#3}$	3.5106(11)	4.403(3)	35.68
C(34)–Br(2)···Cg(6)$^{\#4}$	3.5498(12)	4.932(3)	44.92
#1=1-x,-y,2-z, #2=1-x,-y,1-z, #3=1+x,y,z #4=x,y,-1+z.			
Cg(1)=Ni1–O1–C12–N4–N3, Cg(2)=Ni1–O2–C30–N8–N7, Cg(3)= Ni1–N1–C5–C6–N3, Cg(6)=N2B^B–C7–C11B^B–C8–C9–C10, Cg(7)= N5–C19–C20–C21–C22–C23, Cg(10)=C13–C14–C15–C16–C17–C18 .			

	6		
C(1)–H(1)···Cg(2)	2.95	3.2996(3)	104
C(19)–H(19)···Cg(1)	2.84	3.1518(3)	101
C(16)–Br(1)···Cg(3)$^{\#1}$	3.8388(4)	4.3997(4)	94.21(1)
N(9)–O(4)···Cg(4)$^{\#2}$	3.9686(4)	5.0552(5)	147.57(1)
N(9)–O(5)···Cg(8)$^{\#3}$	3.2502(3)	4.3721(4)	148.68(1)

#1= 1/2+x,1/2-y,-1/2+z, #2 = 1/2+x,1/2-y,1/2+z, #3 = 1/2-x,-1/2+y,3/2-z.

Cg(1)=Ni(1)-O(1)-C(12)-N(4)-N(3), Cg(2)=Ni(1)-O(2)-C(30)-N(8)-N(7), Cg(3)=Ni(1)-N(1)-C(5)-C(6)-N(3), Cg(4)=Ni(1)-N(5)-C(23)-C(24)-N(7), Cg(8) =N(6)-C(25)-C(26)-C(27)-C(28)-C(29).

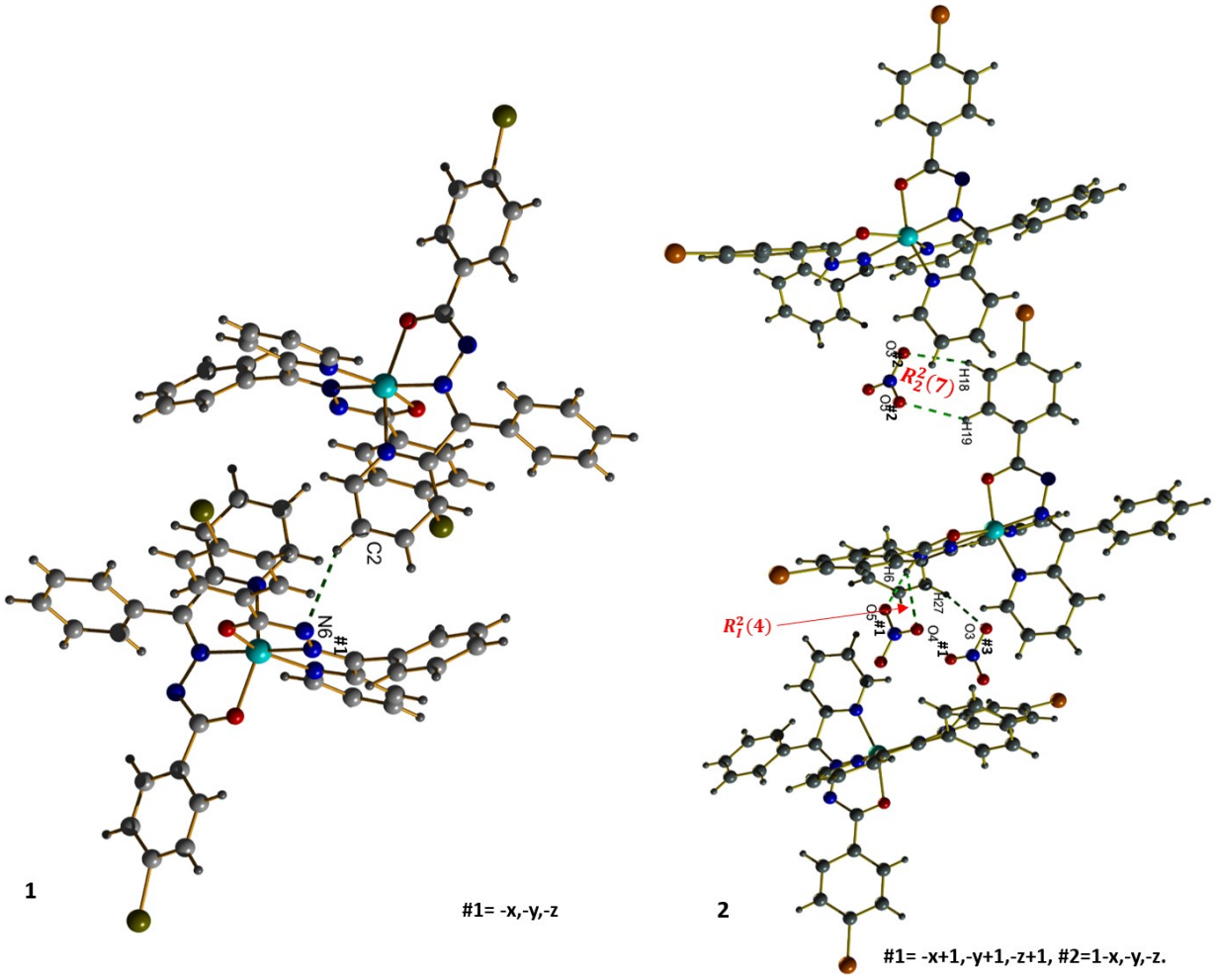

Figure S1. Various intra and intermolecular H-bonding interactions present in complexes **1** and **2**.

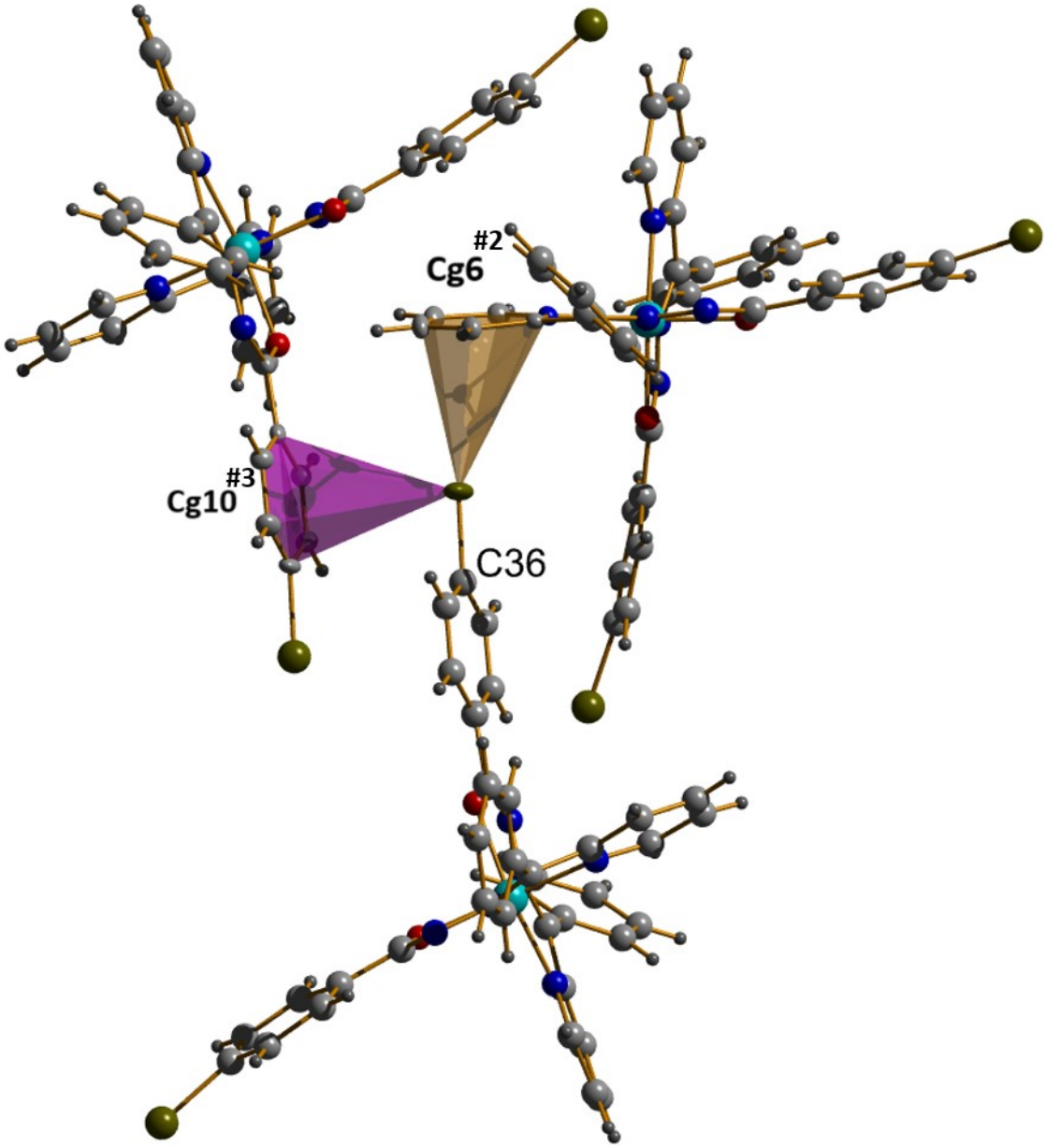

Figure S2. C─Br···π interactions in complex **1.**

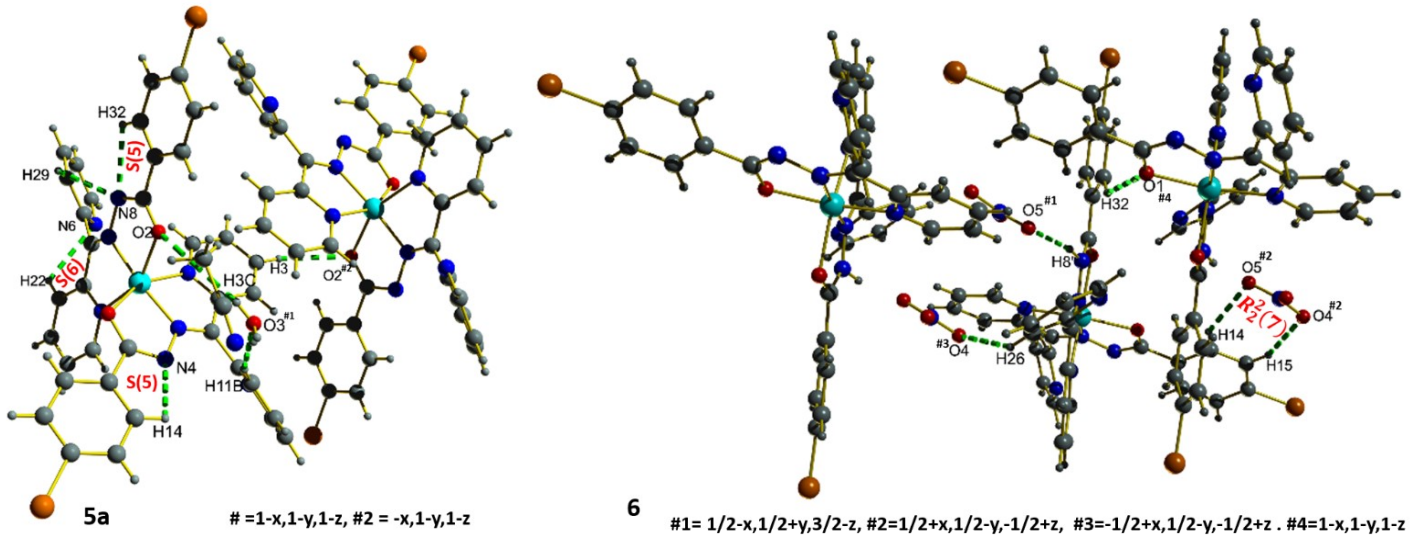

Figure S3. Various intra and intermolecular interactions present in complexes **5a** and **6**.

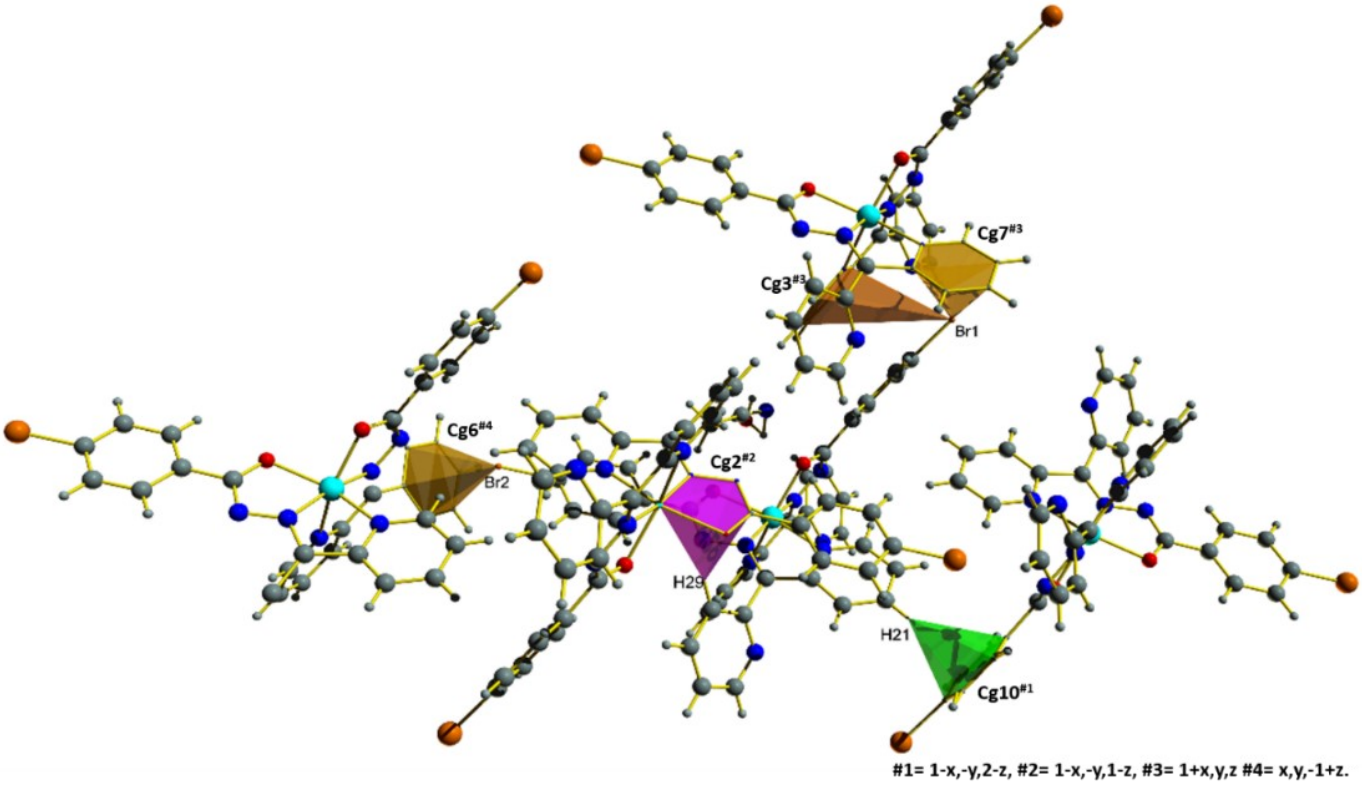

Figure S4. C–H···π and C–Br···π interactions in complex **5a.**

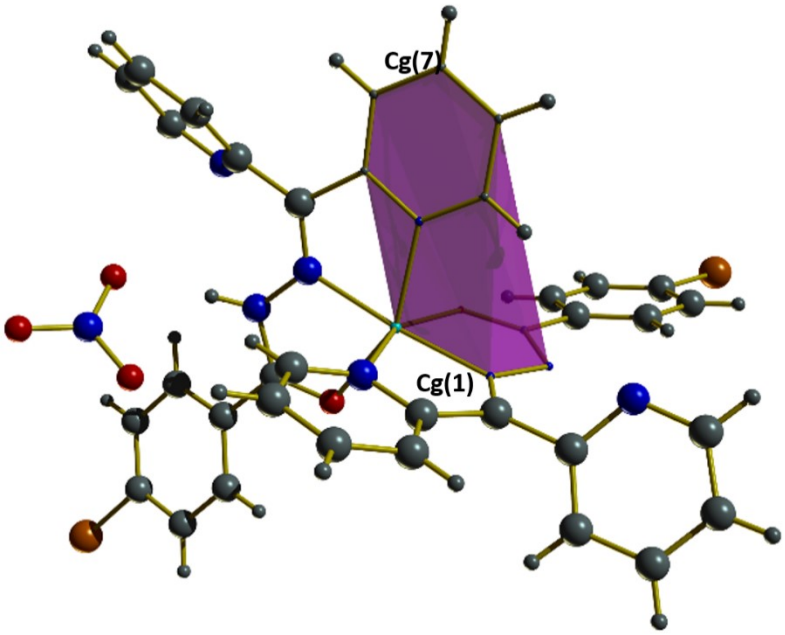

Figure S5. π···π Interactions in complex **6**.

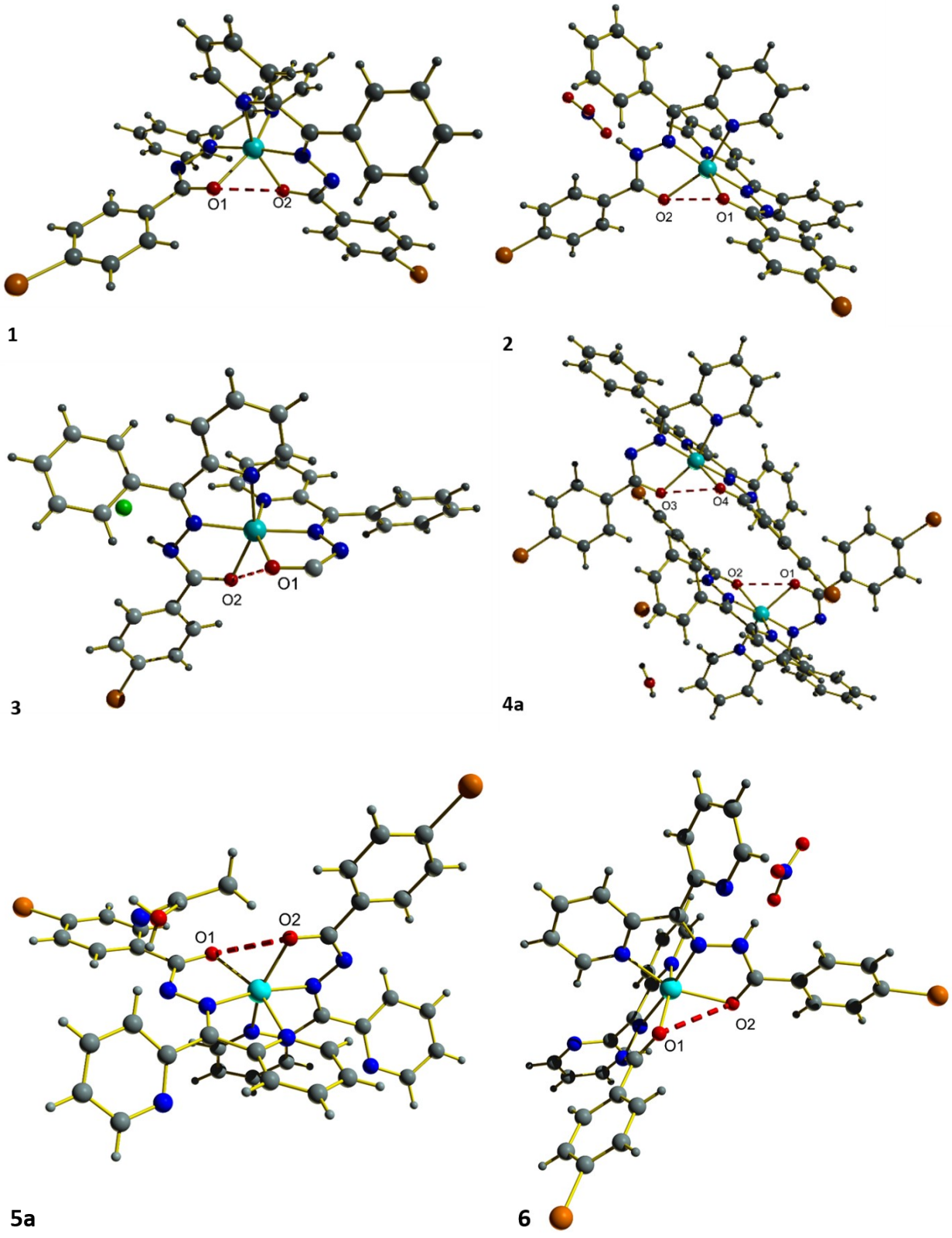

Figure S6. Chalcogen···chalcogen interaction in complexes **1**-**6**.

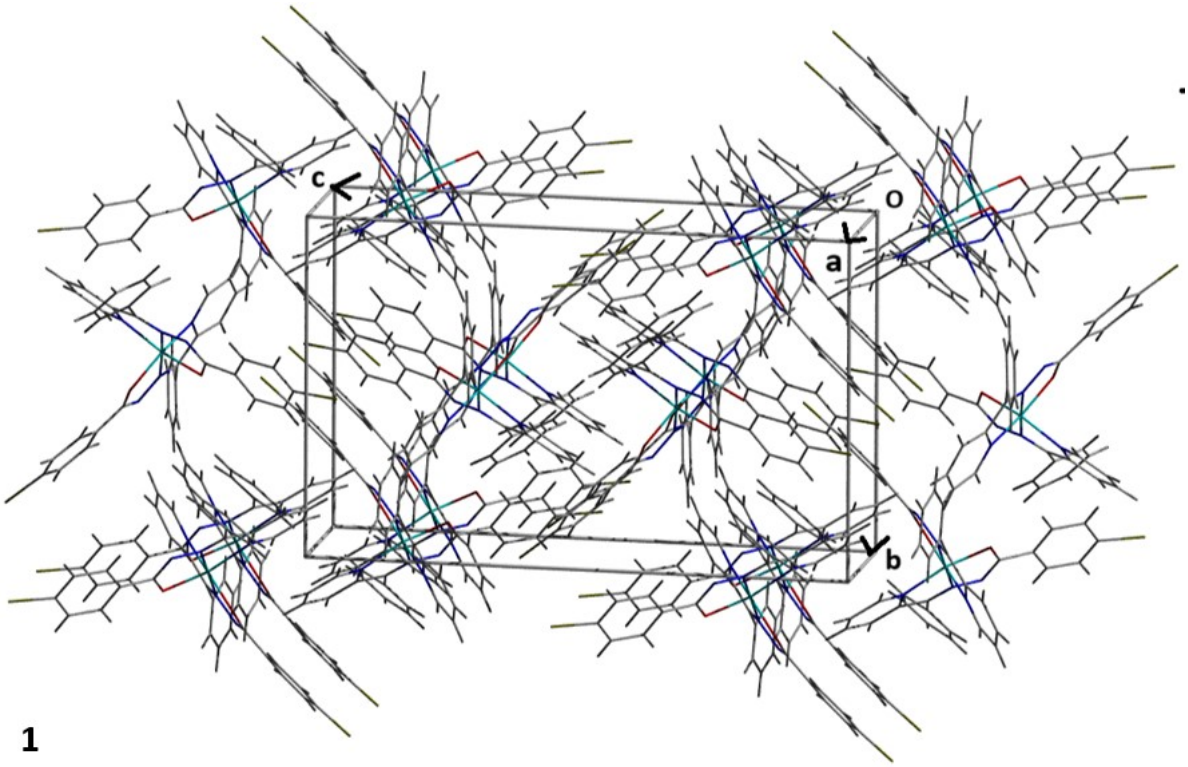

1

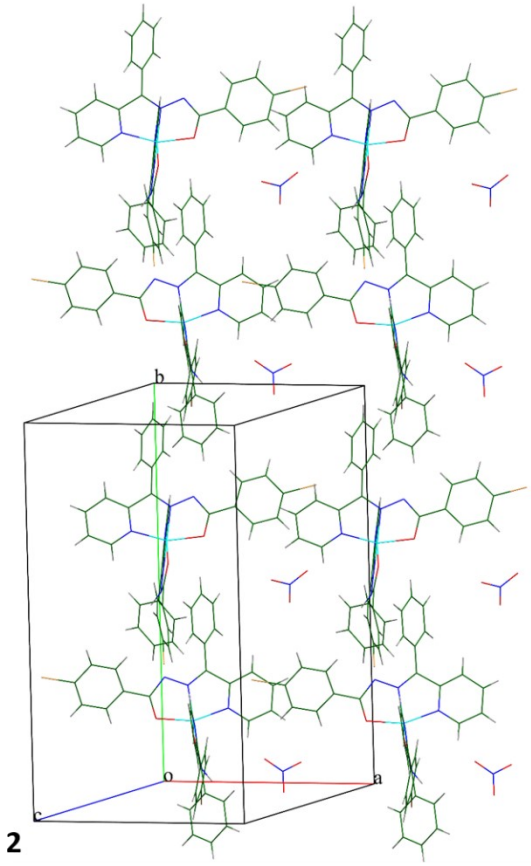

2

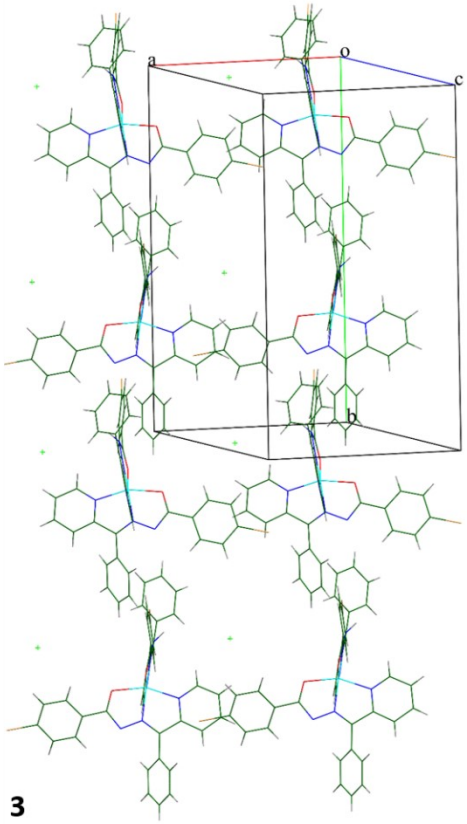

3

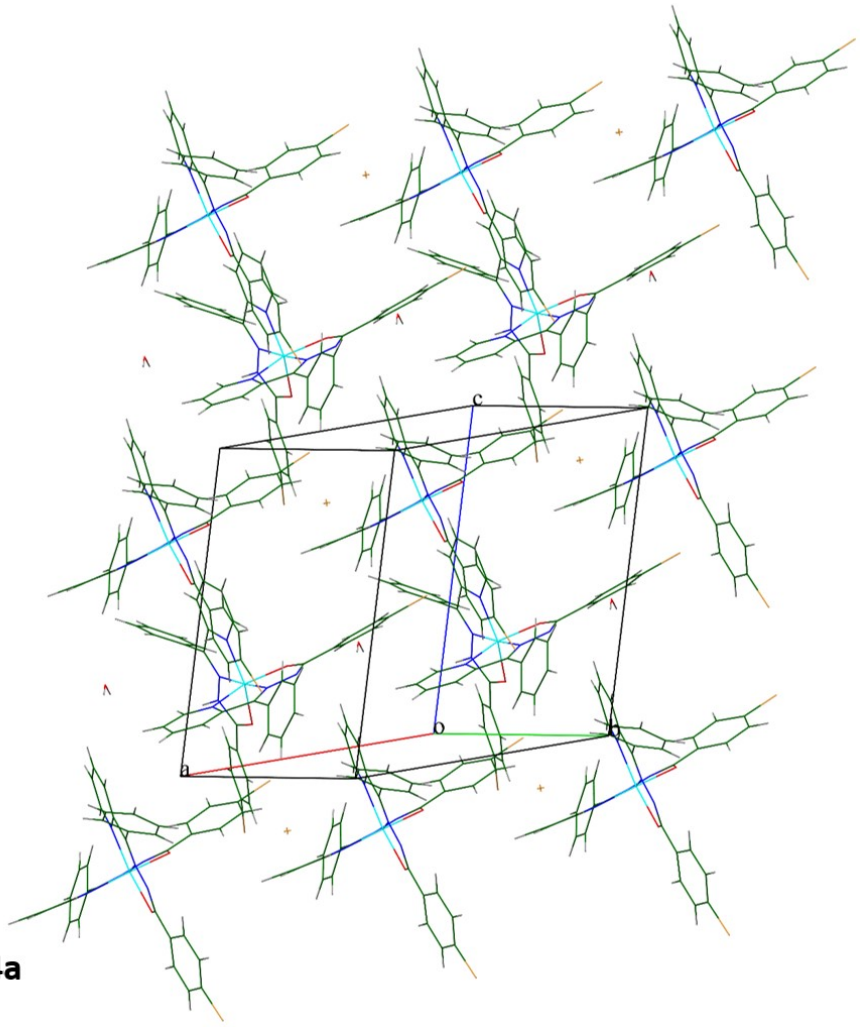

4a

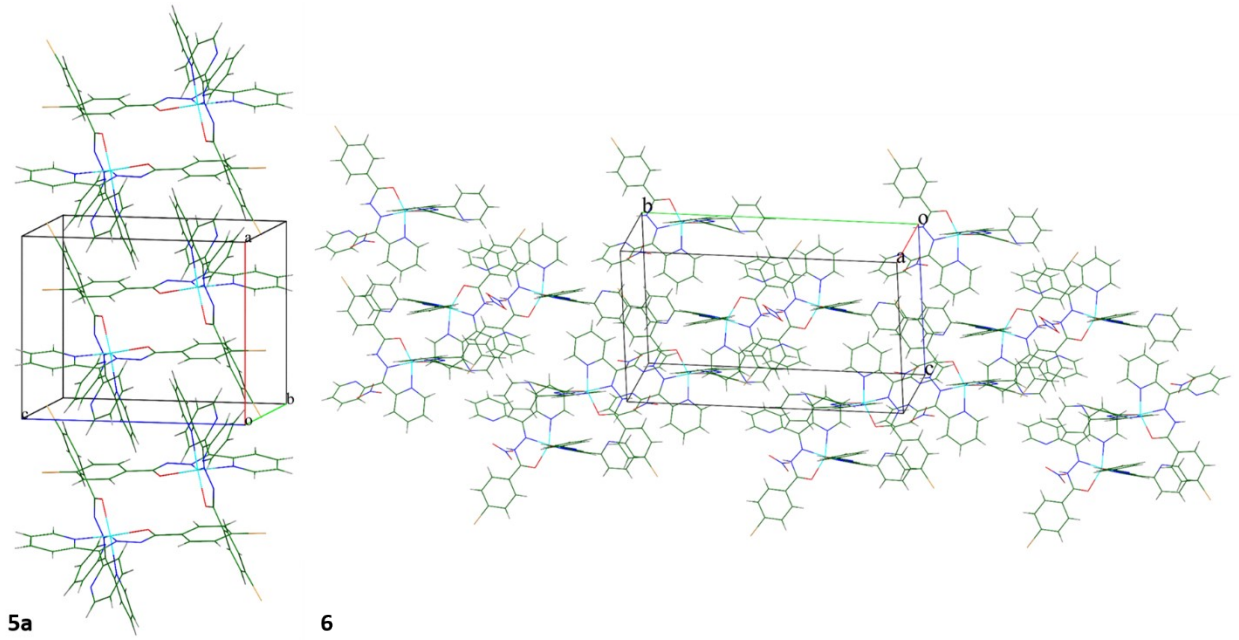

Figure S7. Packing of complexes **1** and **6** along 'bc', (**2**, **3**, **4a** and **5a** along 'ac') plane to form a supramolecular structure *via* various interactions.

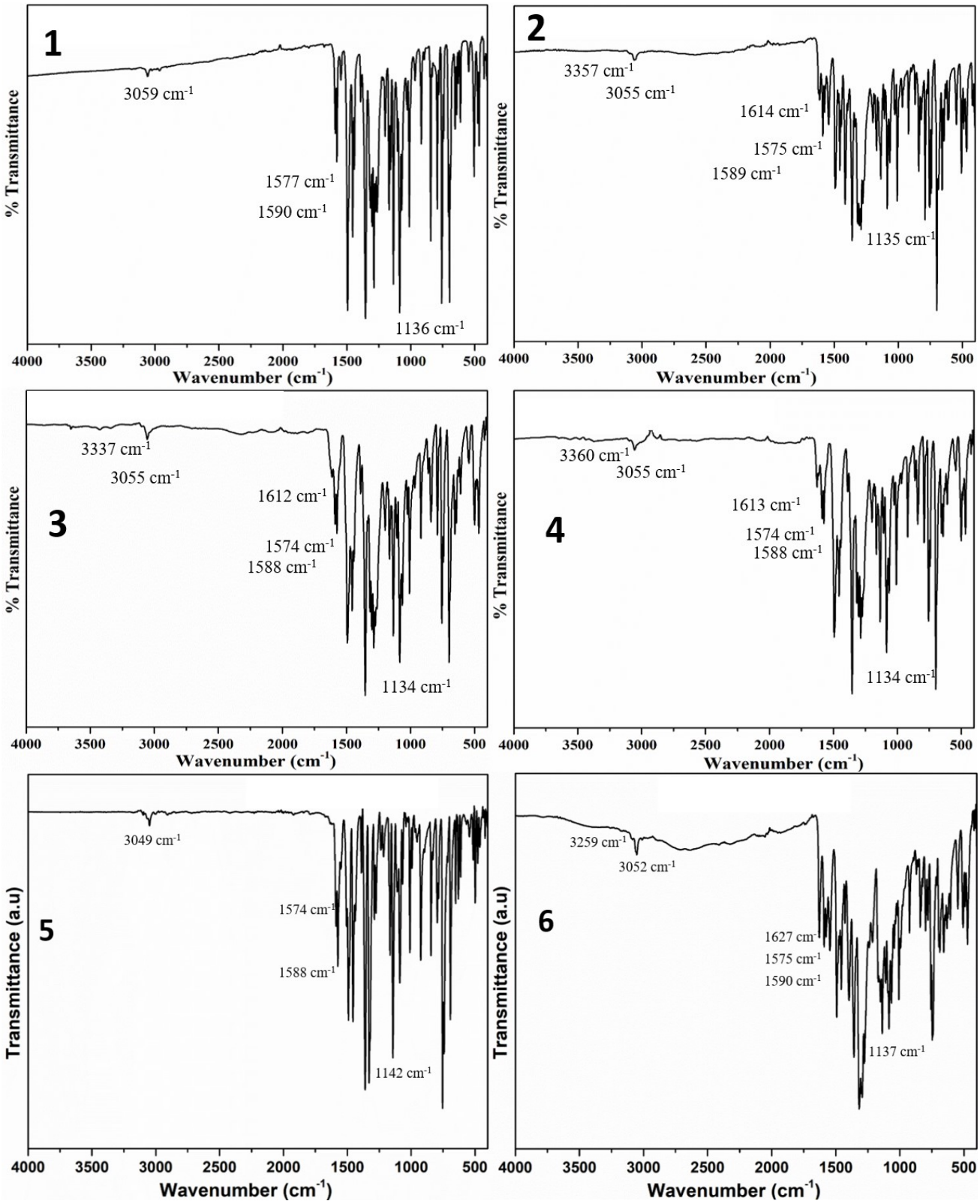
1
3059 cm-1
1577 cm-1
1590 cm-1
1136 cm-1
% Transmittance
2
3357 cm-1
3055 cm-1
1614 cm-1
1575 cm-1
1589 cm-1
1135 cm-1
% Transmittance
3
3337 cm-1
3055 cm-1
1612 cm-1
1574 cm-1
1588 cm-1
1134 cm-1
% Transmittance
4
3360 cm-1
3055 cm-1
1613 cm-1
1574 cm-1
1588 cm-1
1134 cm-1
% Transmittance
5
3049 cm-1
1574 cm-1
1588 cm-1
1142 cm-1
Transmittance (a.u)
6
3259 cm-1
3052 cm-1
1627 cm-1
1575 cm-1
1590 cm-1
1137 cm-1
Transmittance (a.u)
4000 3500 3000 2500 2000 1500 1000 500
Wavenumber (cm-1)

Figure S8. FT-IR spectra of complexes **1-6.**

Table S4. FT IR spectral assignments of aroylhydrazone and their Ni(II) complexes **1-6** in cm^{-1}.

	v(N–H)	v(C=O)/ v(C–O)	v(C=N)	v(C=N)[a]	v(N–N)	v(C–H)
HBpB	3348	1683	1584	----	1133	3058
1	----	1353	1577	1590	1136	3059
2	3375	1614, 1361	1575	1589	1137	3055
3	3337	1612, 1354	1574	1588	1134	3055
4	3360	1613, 1354	1574	1588	1134	3055
HDpB	3334	1673	1585	----	1132	3044
5	----	1360	1574	1588	1142	3049
6	3259	1627, 1358	1575	1590	1137	3052

a) newly formed C=N group

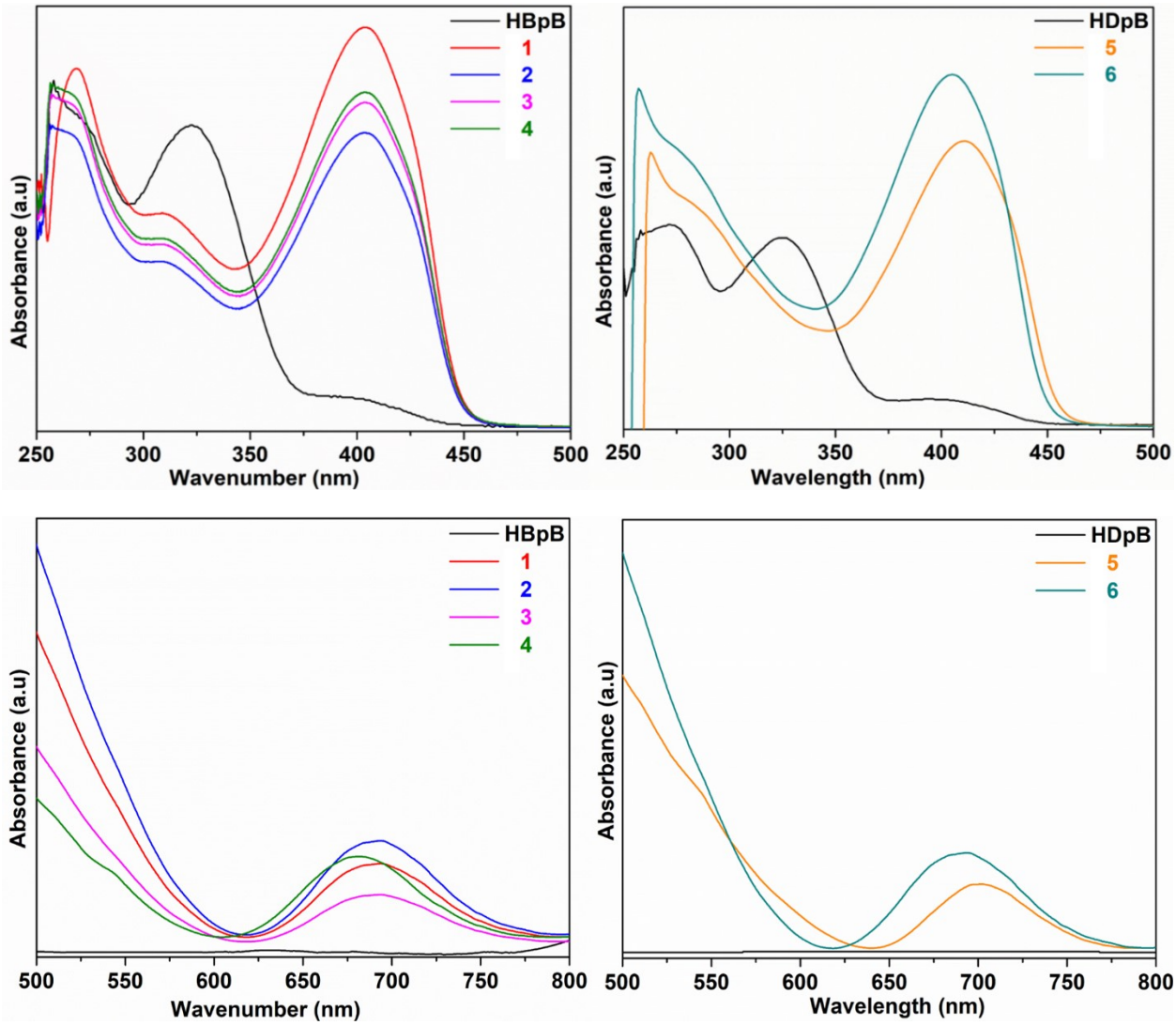

Figure S9. Electronic spectra of complexes **1-6** in DMSO of complexes **1-6** in DMSO.

Table S5.

Compound	Intraligand transitions (nm)	LMCT (nm)	d-d transition (nm)
1	269, 325	404	696
2	265, 311	404	699
3	263, 312	404	705
4	264, 310	404	701
5	257, 295	405	692
6	263, 294	410	700

Electronic spectral assignment (nm) of complexes **1**-**6**.

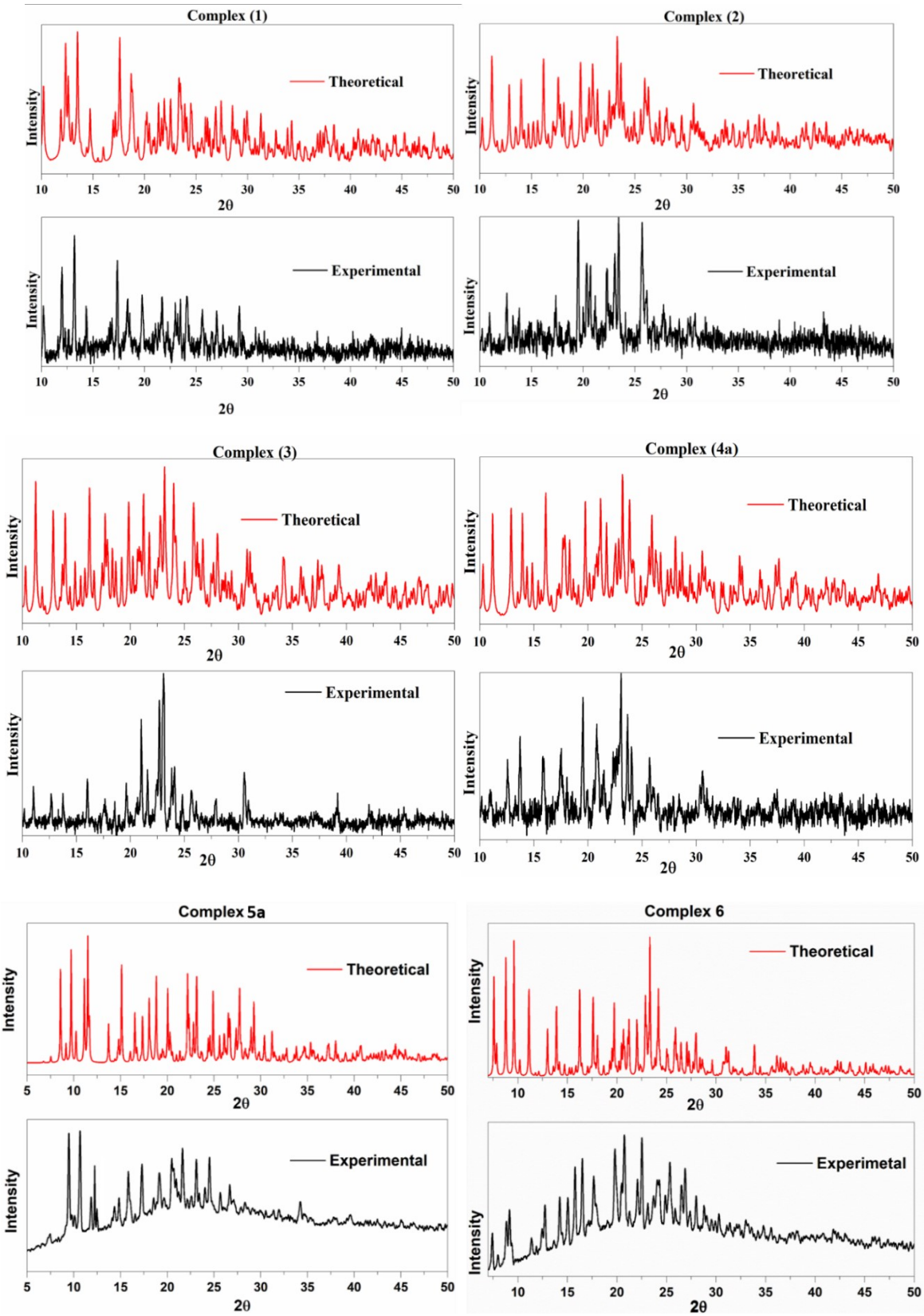

Figure S10. Experimental and theoretical powder XRD patterns of complexes **1-6**.

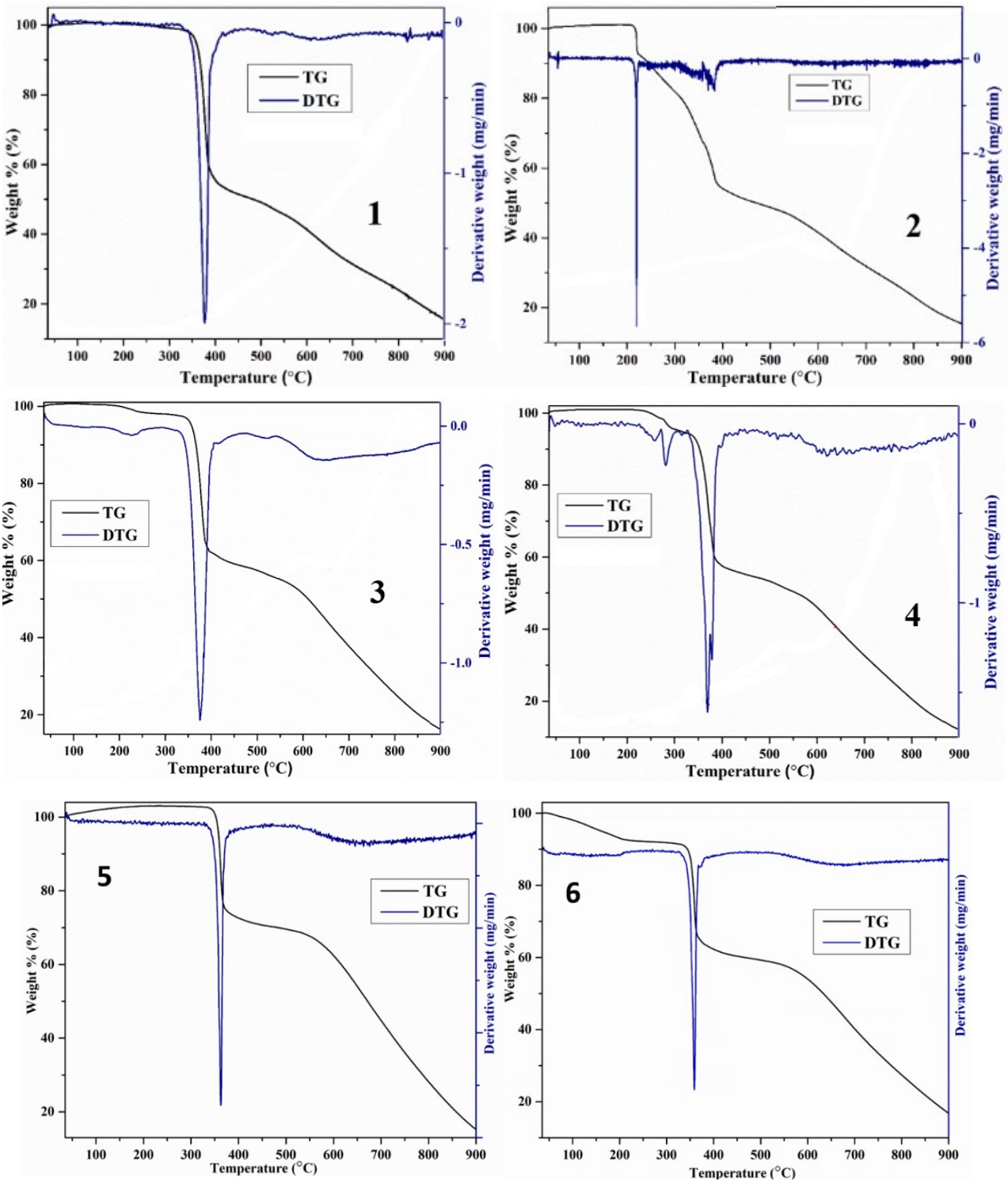

Figure S11. Thermograms of complexes **1-6**.

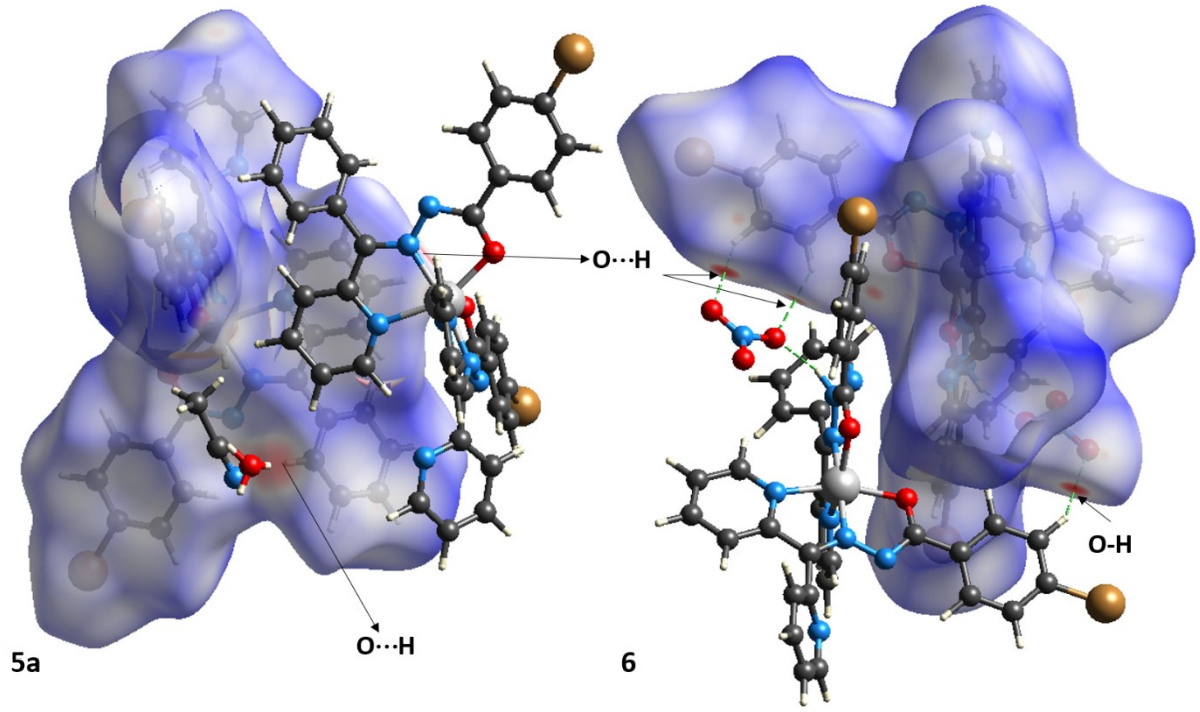

Figure S12. 3D Hirshfeld surface plots with d_{norm} of the complexes **5a** and **6**.

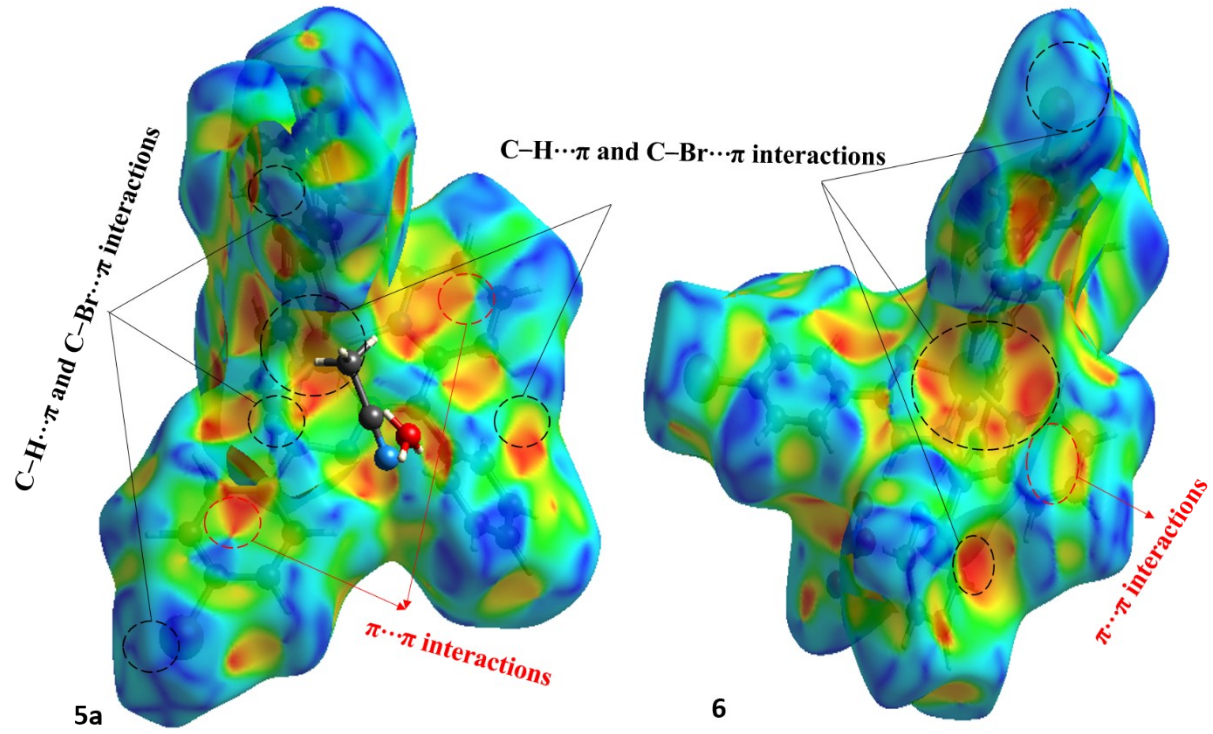

Figure S13. Hirshfeld surface plots with shape index of the complexes **5a** and **6**.

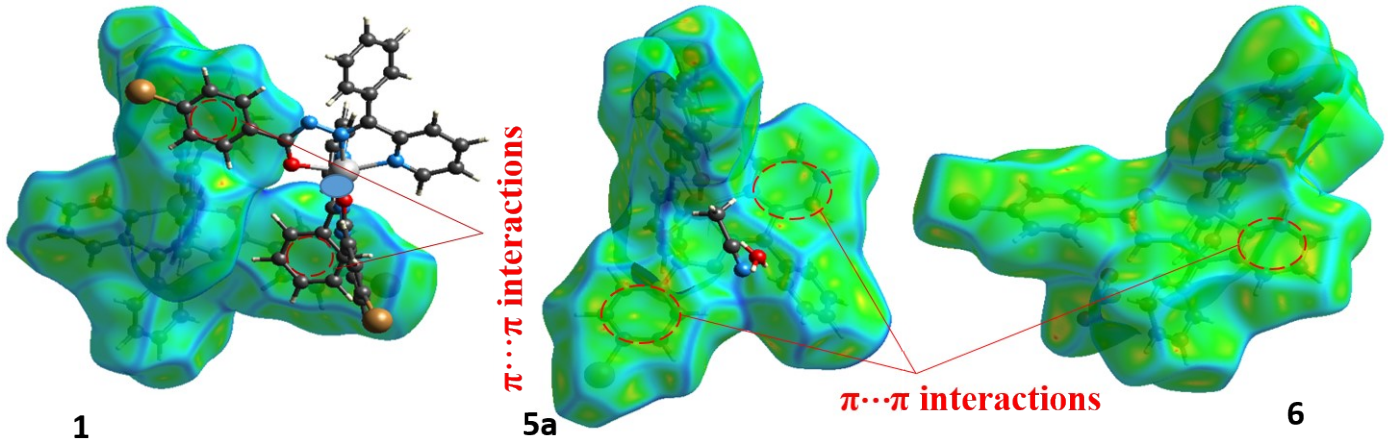

Figure S14. Hirshfeld surface plots with curvedness of the complexes **1, 5a** and **6**.

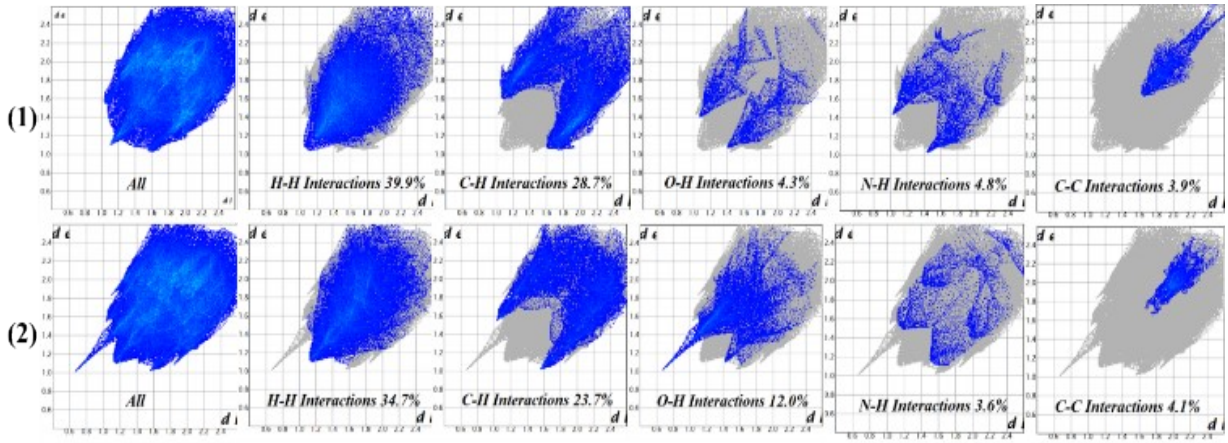

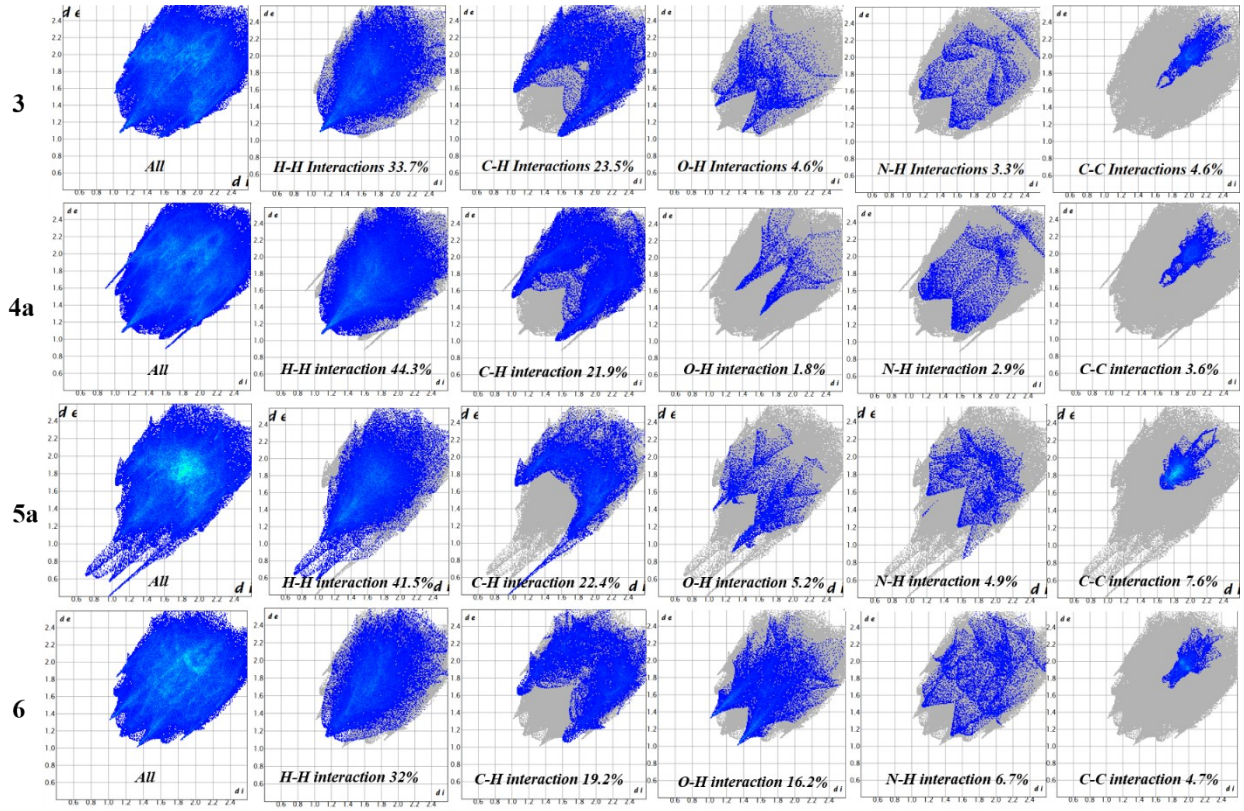

Figure S15. 2D fingerprint plot of major type of interactions in complexes **1-6**.

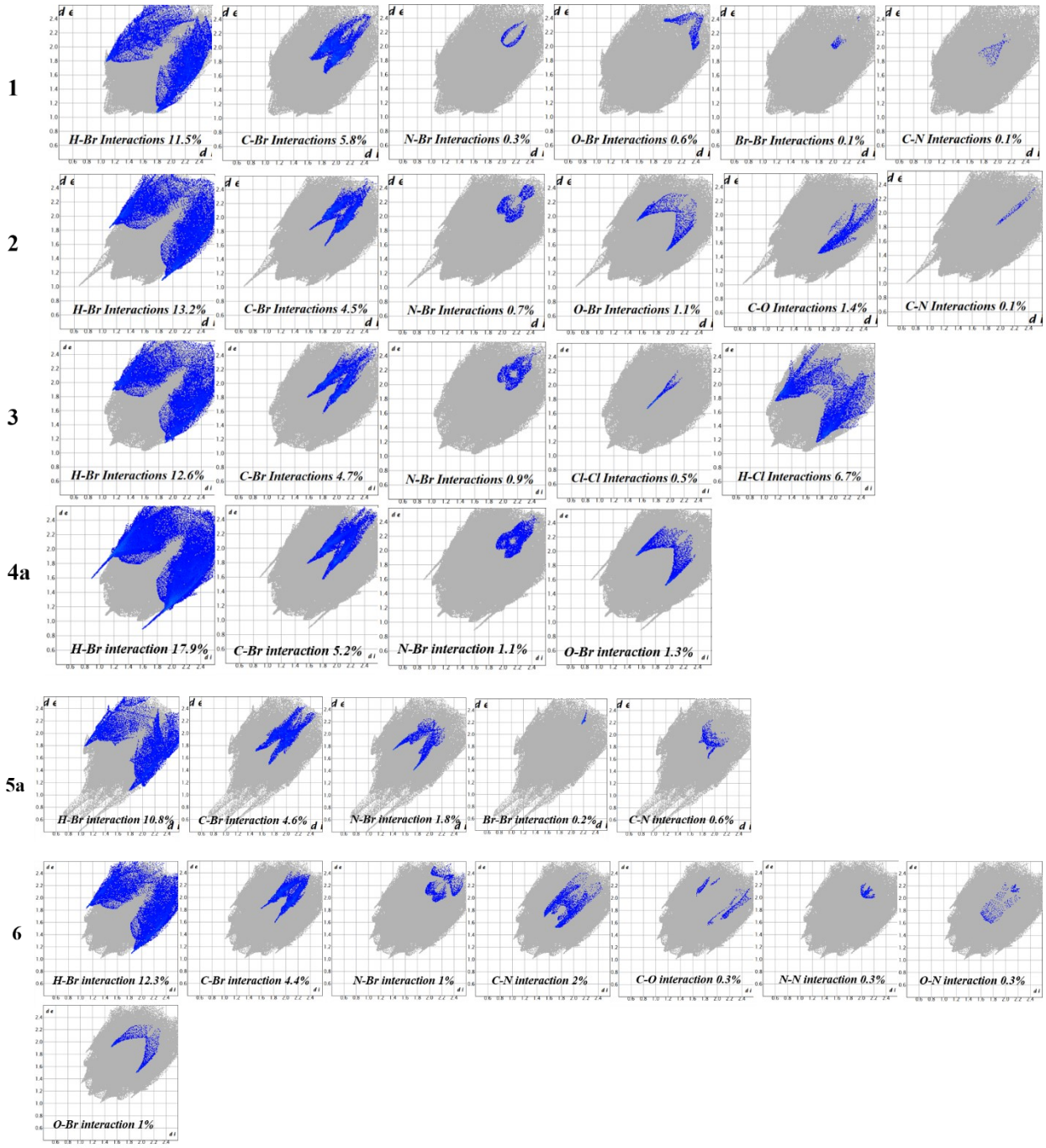

Figure S16. 2D fingerprint plot of other minor type of interactions in complexes **1-6**.

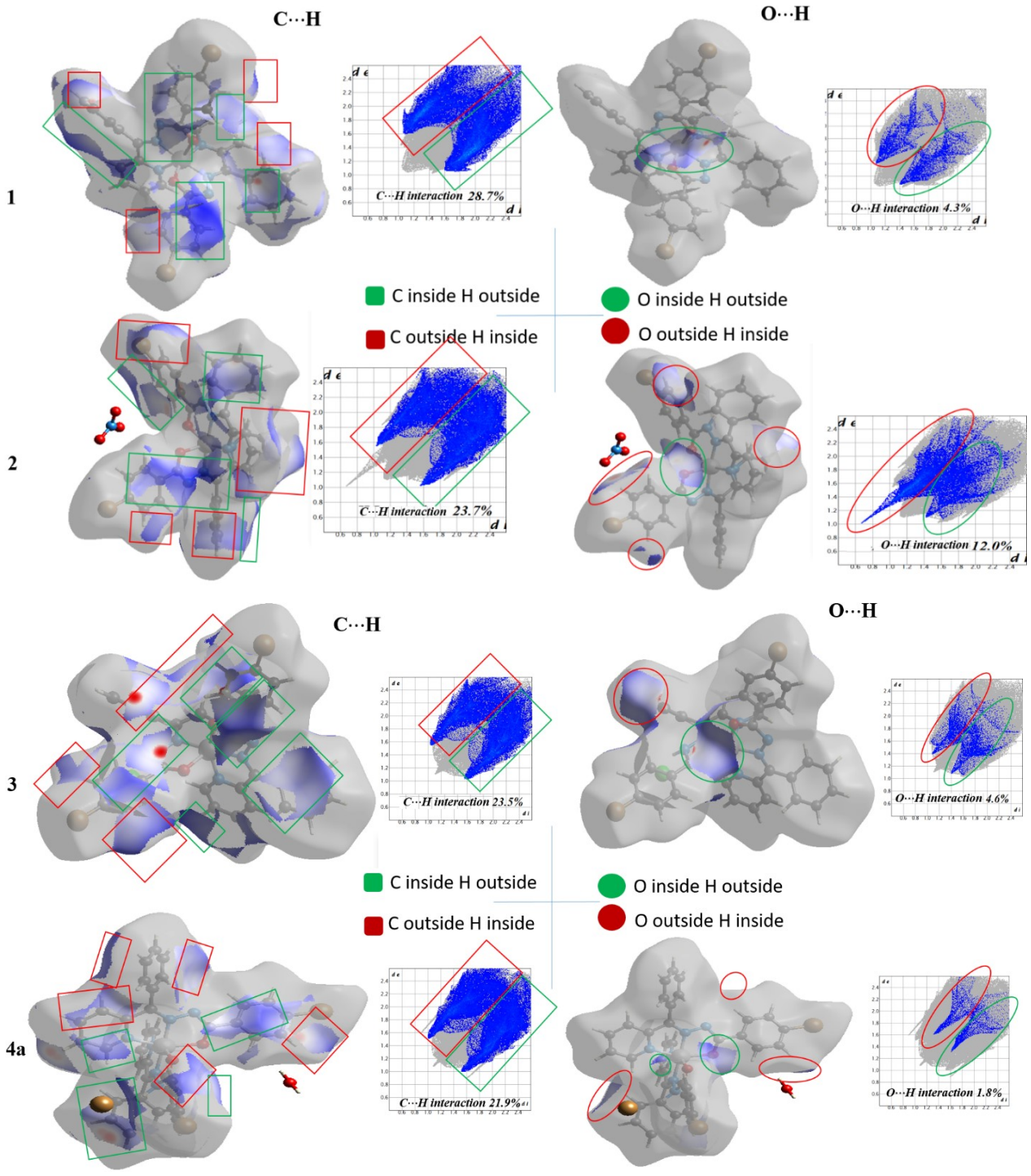
C···H
O···H
1
C···H interaction 28.7%
O···H interaction 4.3%
C inside H outside
C outside H inside
O inside H outside
O outside H inside
2
C···H interaction 23.7%
O···H interaction 12.0%
C···H
O···H
3
C···H interaction 23.5%
O···H interaction 4.6%
C inside H outside
C outside H inside
O inside H outside
O outside H inside
4a
C···H interaction 21.9%
O···H interaction 1.8%

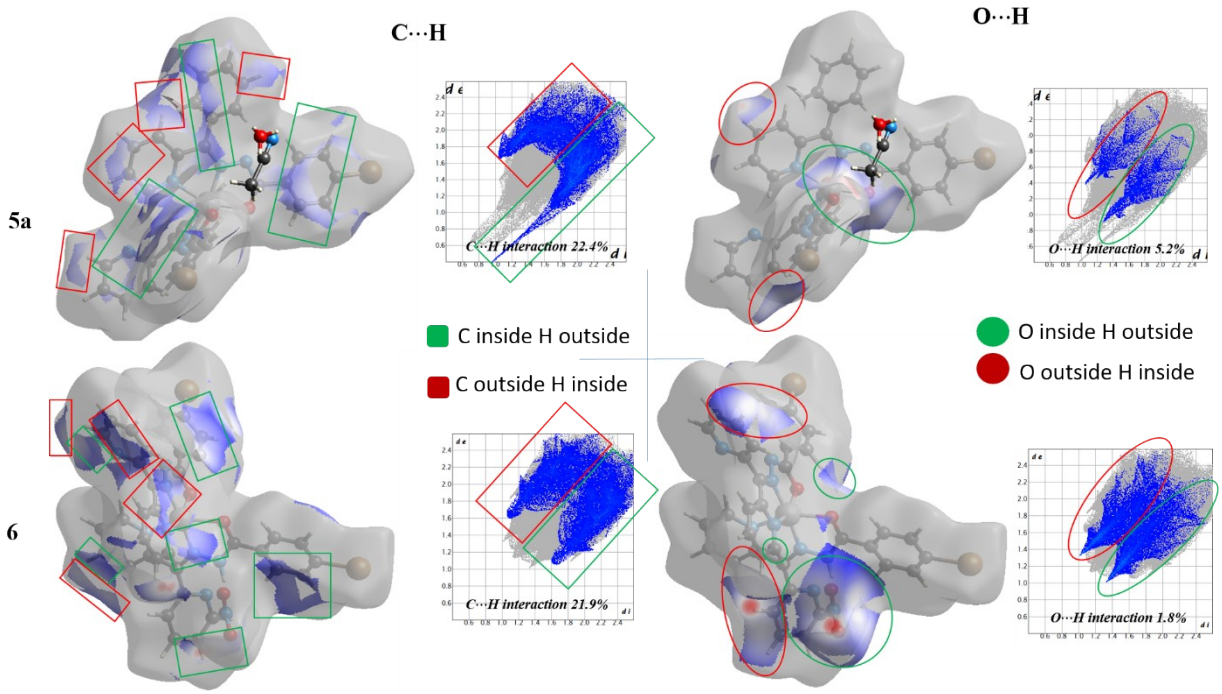

Figure S17. C···H and O···H interactions present in **3 -6** with associated surface patches.

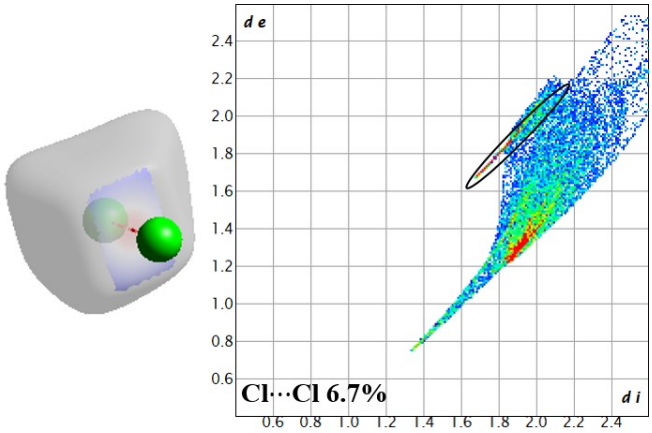

Figure S18. 2D fingerprint plot and HS surface of chlorine-chlorine interactions in **3**.

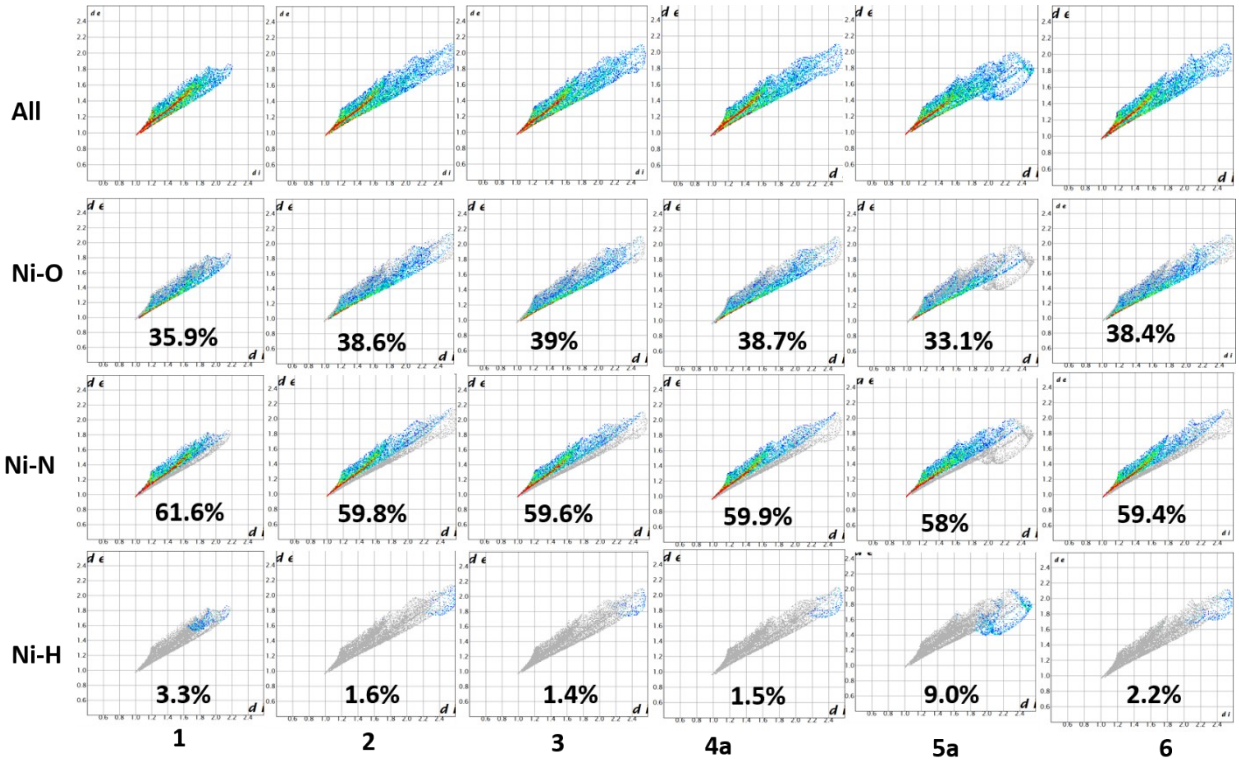

Figure S19. View of the 2D fingerprint plots for the nickel centers corresponding to all, Ni···O, Ni···N and Ni···H interactions in **1**-**6**.

Table S6. Quantitative data from the Hirshfeld surface for the nickel center in **1**-**6**.

Complex	V_H (Å^3)	A_H (Å^2)	G	Ω
1	10.78	30.10	0.784	0.016
2	11.58	32.43	0.763	0.037
3	11.52	32.34	0.763	0.035
4a	11.17	31.46	0.768	0.036
5a	12.26	33.38	0.770	0.056
6	11.56	32.12	0.770	0.036

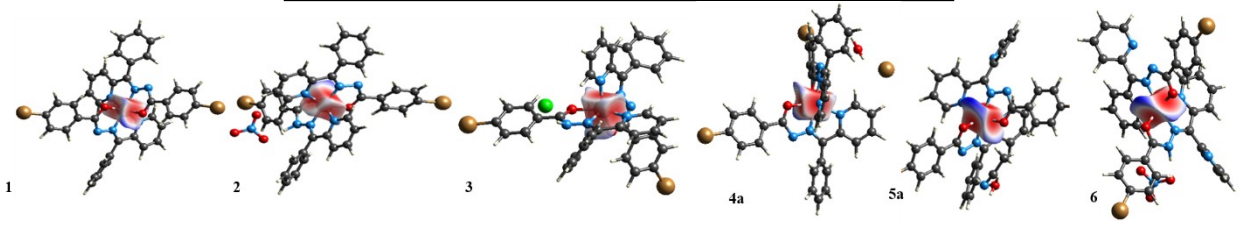

Figure S20. View of the Hirshfeld surfaces (d_{norm}) for the nickel centers in **1**-**6**.

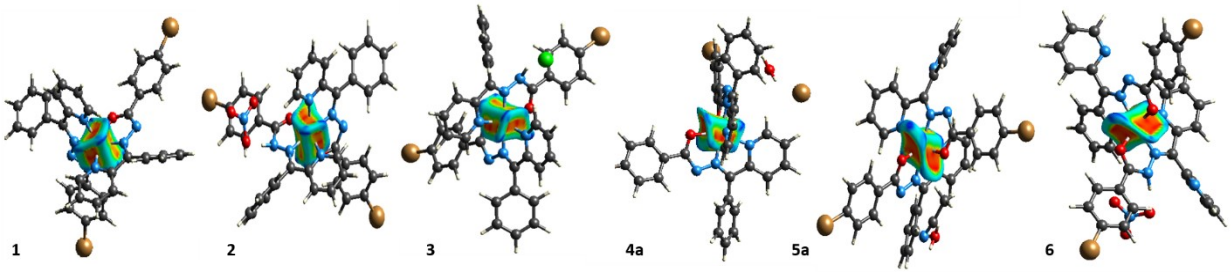

Figure S21. View of the Hirshfeld surfaces (shape index) for the nickel center in **1**-**6**.

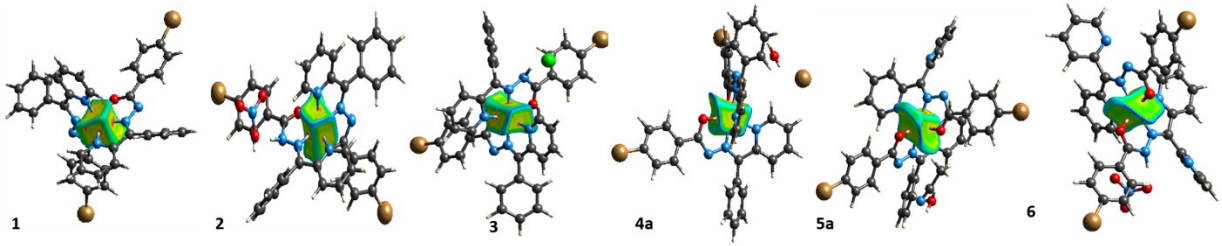

Figure S22. View of the Hirshfeld surfaces (curvedness) for the nickel center in **1**-**6**.

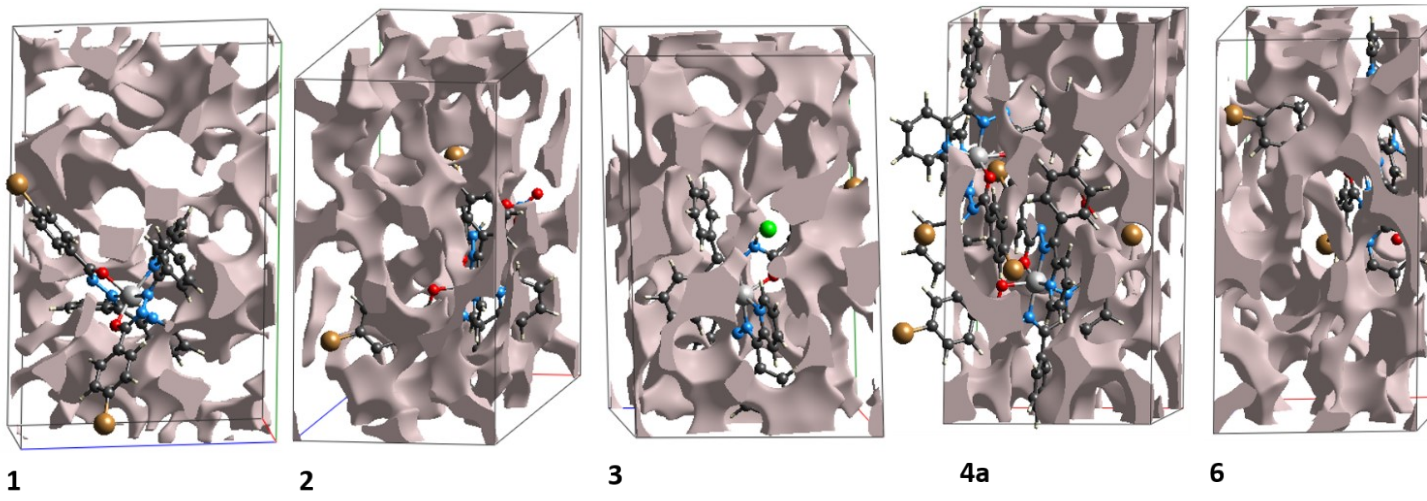

Figure S23. Void surfaces resulting from the iso values of 0.002 au for a unit cell of **1**-**4a** and **6**.

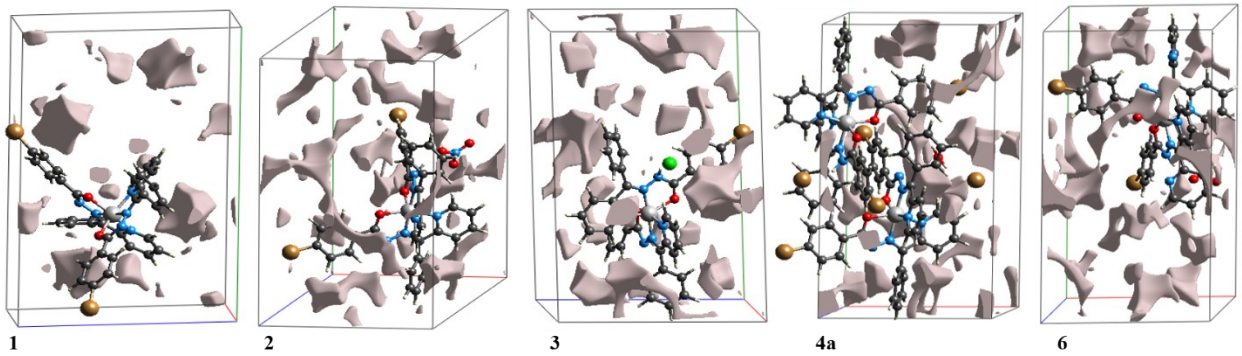

Figure S24. Void surfaces resulting from the iso values of 0.0008 au for a unit cell of **1**-**4a** and **6**.

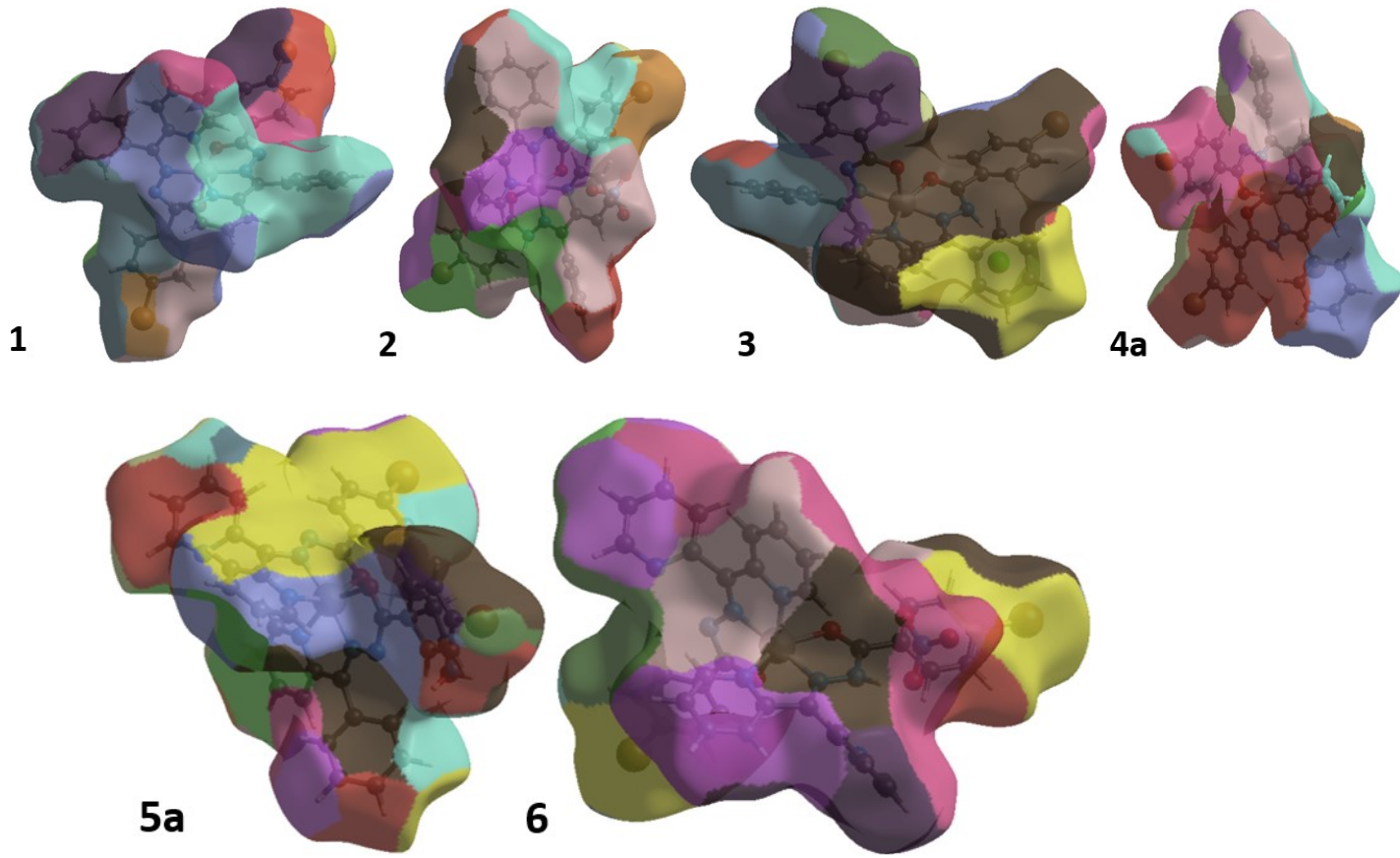

Figure S25. Fragment patch plot of complexes **1-6**.

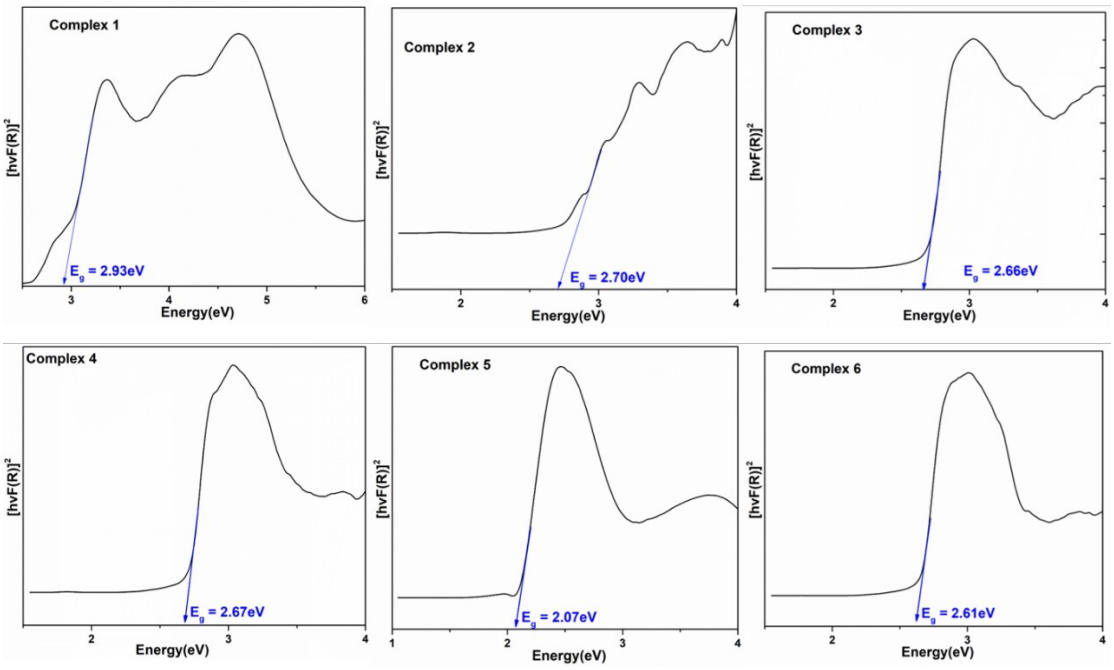

Figure S26. UV-Vis diffuse reflectance spectrum of the complexes **1-6**. The inset shows the band gap from Kubelka-Munk as a function of energy (eV).

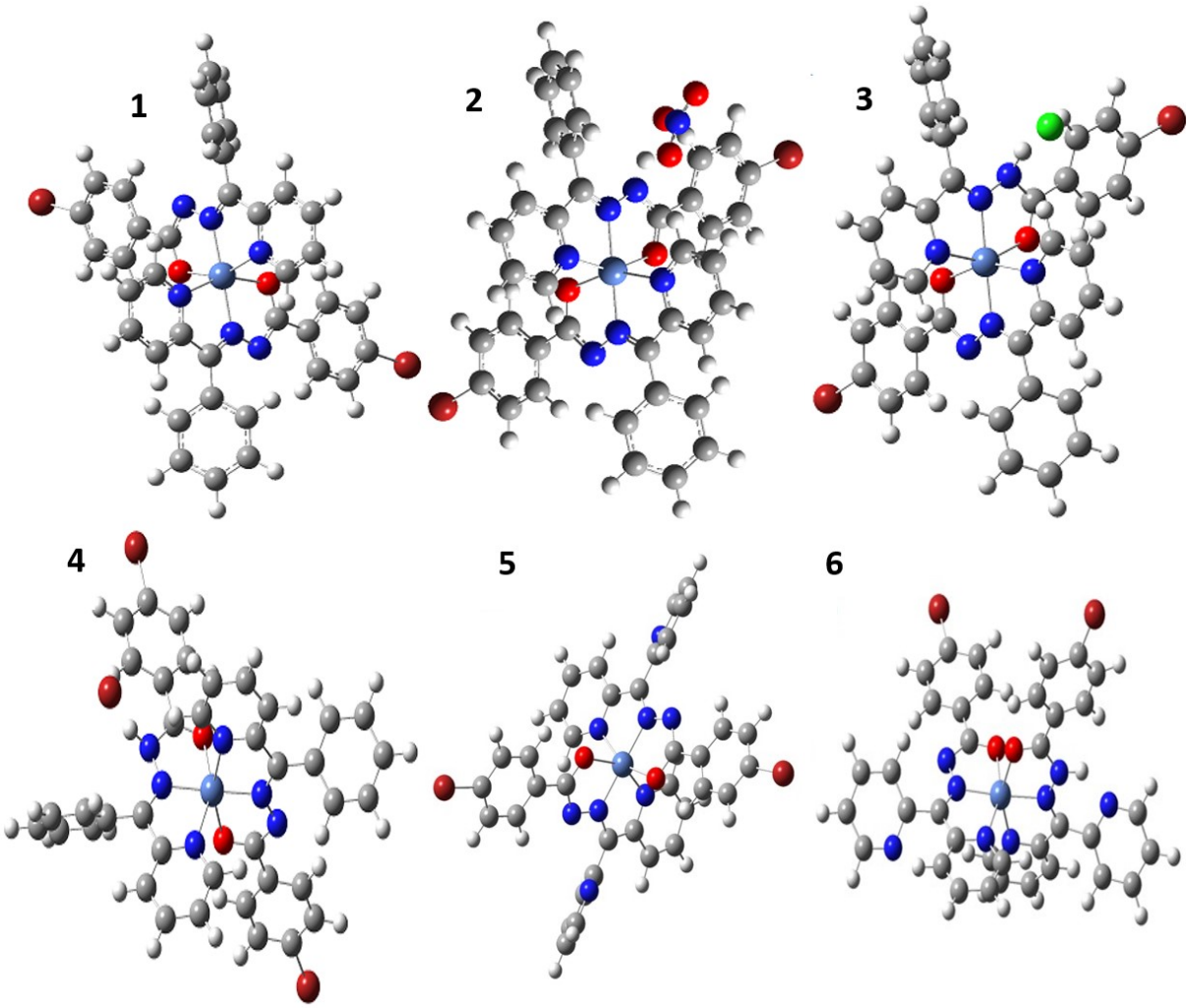

Figure S27. Optimized geometry structures of **1**-**6**.

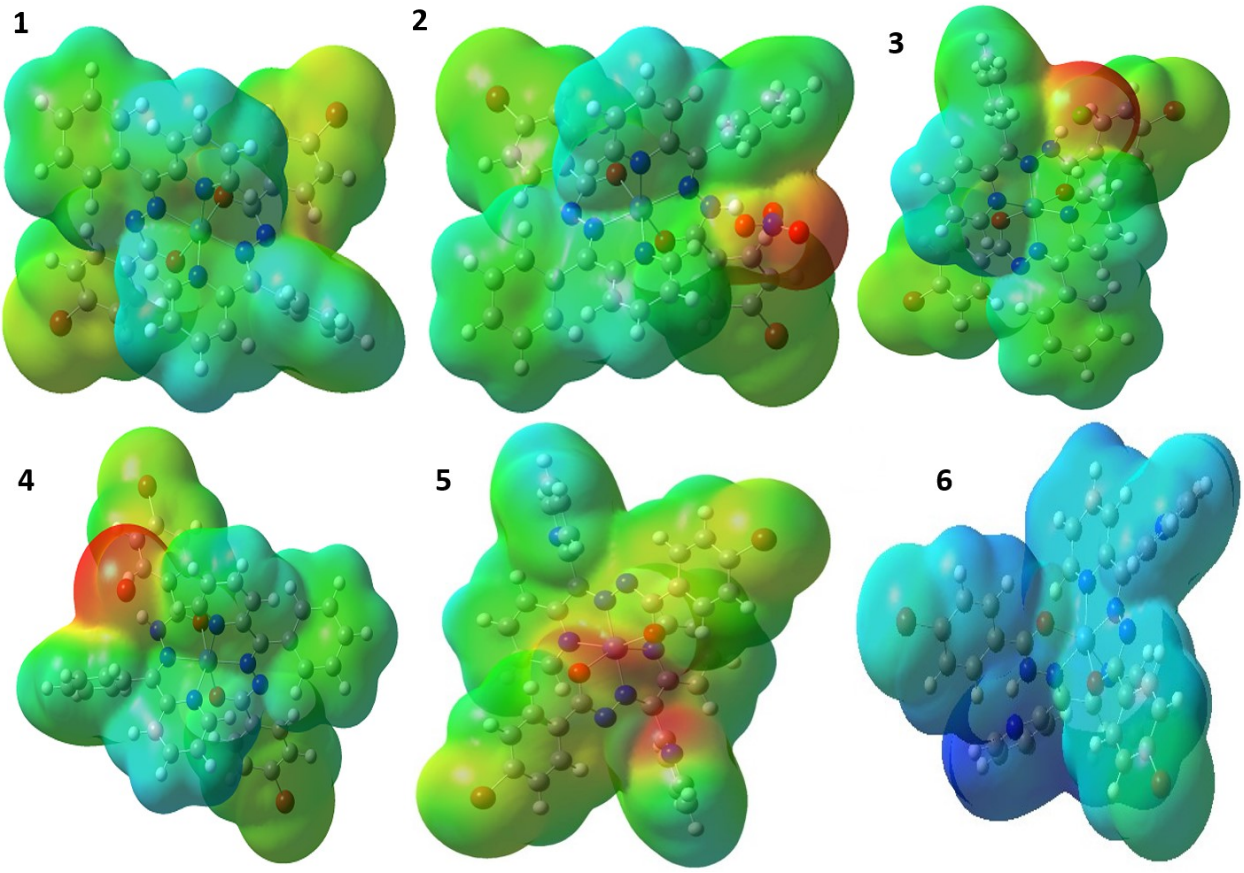

Figure S28. MEP diagram of **1**-**6**.

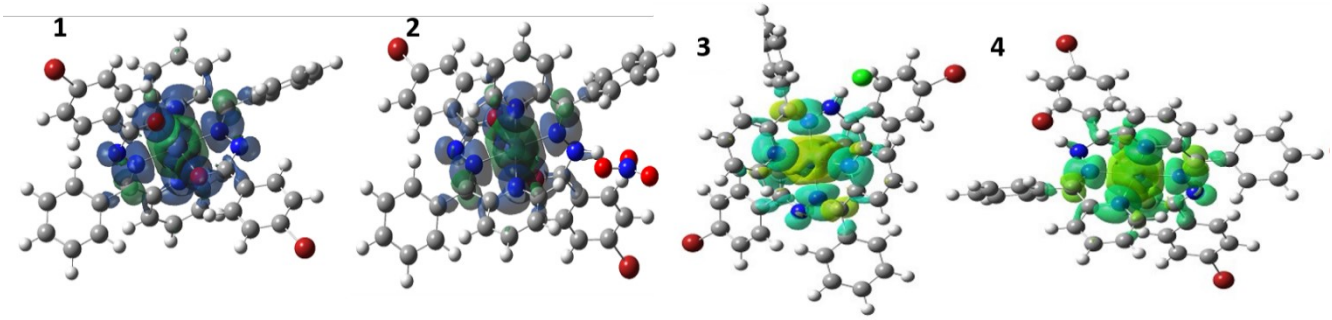

Figure S29. spin density distribution of the complex **1**-**4**.

Table S7. Docking energies and molecular interactions of the complexes with duplex DNA and SARS-CoV-2 targets.

PDB ID.	Compound	Docking energy(kcal/mol)	Hydrogen bonding	Residues involving hydrophobic and other interactions
1BNA	**N1**	-9.0	A:DC11:C4'-O1, B:DC3:C1'-Br1	----
	N2$^+$	-8.1	----	A:DG12:OP2-phenyl1, A:DG12:C5' -:Phenyl1
	N5	-9.1	A:DC11:C4'-O1	A:DC11:OP1–pyridine1, A:DG12:OP1-Phenyl2, A:DG12:OP1-pyridine3,
	N6$^+$	-8.9	A:DC3:H41–pyridine2	B:DA6:OP2–pyridine4, A:DC3:C5-pyridine2, A:DC3-pyridine2, A:DG4–pyridine1
6Y2F	**N1**	-9.2	A:TYR101:HH-O1	A:LYS88:NZ–phenyl1, A:ASP33:OD2–pyridine2, A:GLU178:OE1–phenyl1, A:TYR101–pyridine1, Br1-A:LYS90
	N2$^+$	-8.8	A:THR199:HG1-O2, A:ASN238:HD21-N3, A:THR196:CA-Br1	A:ARG131:NH2-pyridine2
	N5	-9.4	----	Br1-A:MET276, Br1-A:LEU287, Pyridine2-A:LEU286, phenyl1-A:LEU287
	N6$^+$	-10.1	A:THR199:HG1-O2, A:ASN238:HD21-N4, A:THR196:CA –Br1, A:ASP197:HN–phenyl1	A:ARG131:NH2–pyridine3

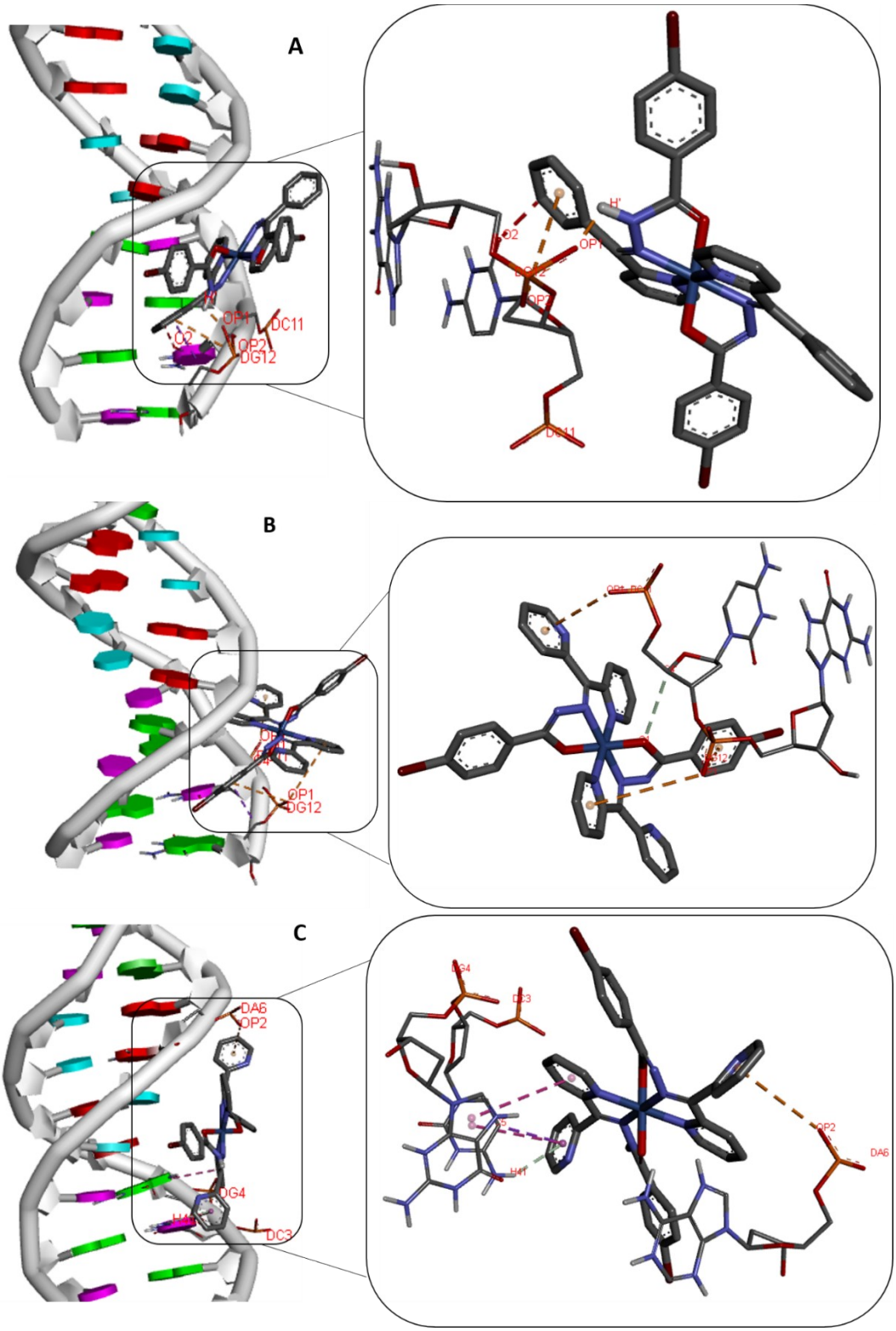

Figure S30. Molecular docking interactions of (A) complex **2** ion, (B) complex **5a** and (C) complex **6** ion with 1BNA.

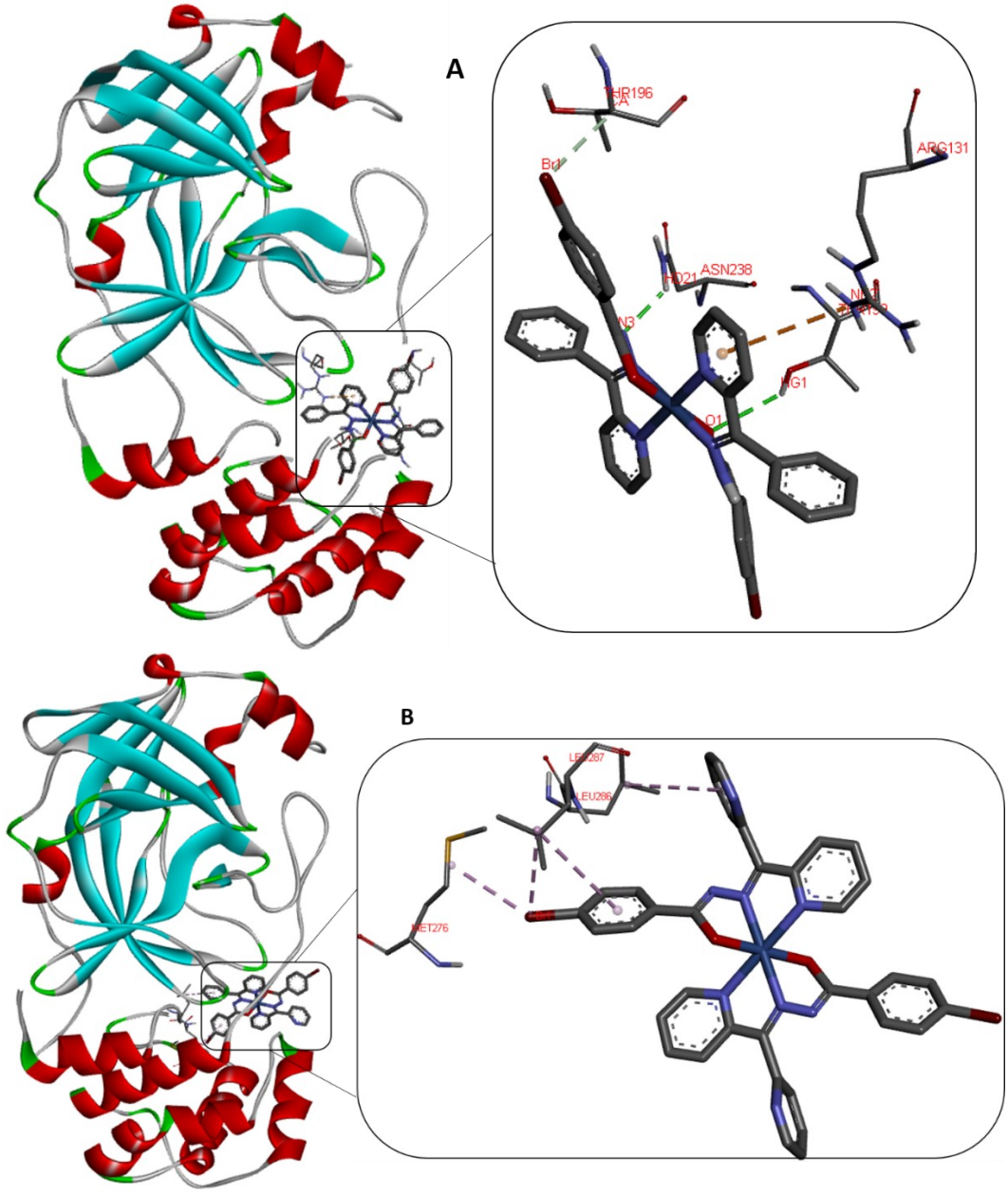
A
THR196
Br1
ARG131
HD21
ASN238
N3
HG1
O1
B
LEU287
LEU286
MET276

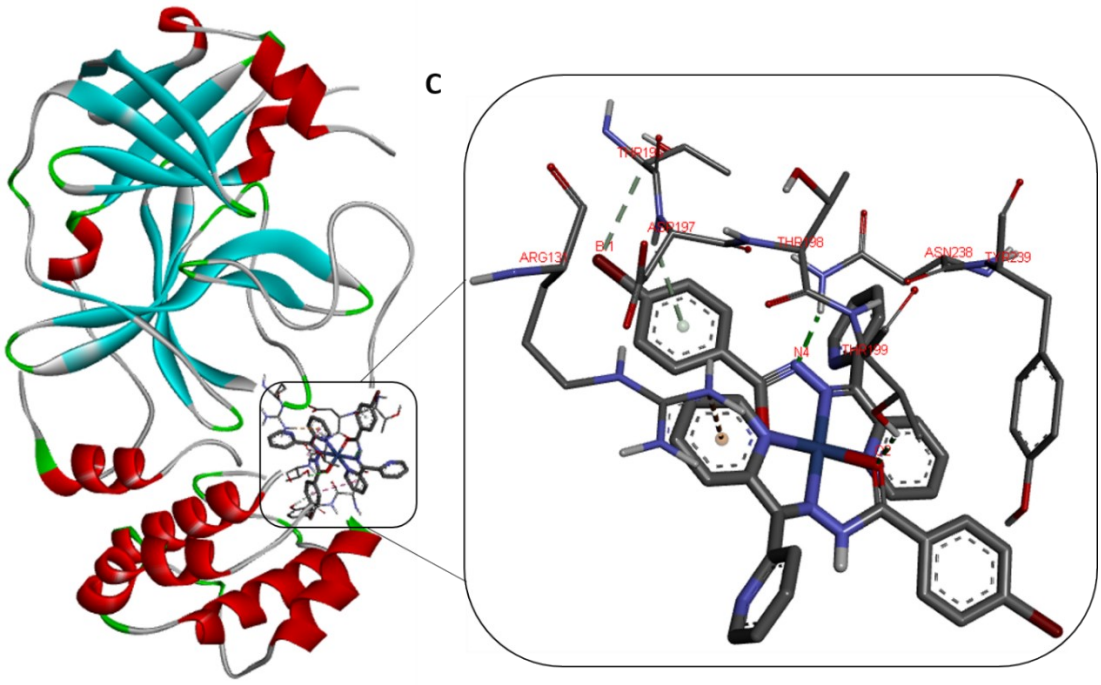

Figure S31. Molecular docking interactions of (A) complex **2** ion, (B) complex **5a** and (C) complex **6** ion with SARS-CoV-2 target.

References

1. P. K. Maniyampara, M. Bhagiyalakshmi, M. R. P. Kurup, E. Manoj and K. K. Damodaran, *J. Mol. Struct.*, 2024, **1318**, 139214.